Robust tuning of multivariable systems
with decentralized control and decouplers

FINAL YEAR PROJECT

Author
Anders Willersrud
December 17, 2009

Supervisor
Professor Morten Hovd

Co-supervisors
Professor Sigurd Skogestad
PhD. Mohammad Shamsuzzoha

Department of Engineering Cybernetics
Faculty of Information Technology, Mathematics
and Electrical Engineering
Norwegian University of Science and Technology (NTNU)

Abstract

In this report, the objective is to study how to tune PI controllers in a decentralized control structure for multivariable systems. Robustness with respect to (i) parameter changes, (ii) multivariable interactions including opening and closing other loops and (iii) input saturation are tuning criteria. The SIMC tuning rules are extended to the proposed 'robust' SIMC settings which takes expected worst case operation into account. Use of decouplers to maintain the robustness criteria are also discussed as well as tuning of the PI controllers when the decouplers are added to the control scheme.

The proposed techniques are first tested on a simple multivariable system, thereafter an analytic model of a high pressure vessel is derived and the controllers are designed first for SISO cases and then for the complete multivariable vessel.

Based on the different simulations, the proposed robust settings manage to control the systems in a satisfactory manner, both in the nominal case and in the worst case. Combined with a one-way decoupler all of the robustness criteras are met.

Preface

This is the report for my final year specialization project at Norwegian University of Science and Technology (NTNU). The project has been carried out at the Department of Engineering Cybernetics and is a part of my Master's degree in Engineering Cybernetics. The project has been motivated by ABB Integrated Operations, and the problem formulation has been formulated by Dr. ing. Olav Slupphaug at ABB together with Professor Sigurd Skogestad.

Discussions with Professor Sigurd Skogestad has been greatly appreciated and has lead to several of the solutions in this project. Also, discussions with PhD. Mohammad Shamsuzzoha have helped me getting insight and understanding of different tuning rules.

Trondheim, December 2009
Anders Willersrud

Contents

List of Figures

Chapter 1

Introduction

1.1 Motivation

With a continuous increase in computational capacity in computers, the advanced model predictive control (MPC) scheme is applied in more and more applications. Especially in the process industry, MPC is increasing its installation base (Maciejowski, 2002). Nevertheless, traditional controller schemes as the decentralized controller structure with individual PID controllers is still an important topic. Often the MPC resides in a control layer above the PID controllers where the outputs from the MPC is used as setpoints to the PID controllers. Many process plants can have thousands of control loops, and if MPC is installed, only a selected set of control variables and manipulated variables are used. It is therefore still an important issue how to tune the PID controllers.

Even if a controller is tuned to have a desired response to setpoint changes and with a small disturbance rejection, changes in conditions in the process can make the controller perform poor or even make the process unstable. In Seborg et al. (2004) a system is defined as *robust* if it provides satisfactory performance for a wide range of process conditions and for a reasonable degree of model inaccuracy. For smaller multivariable systems, installation of a model predictive controller can be too costly. Yet, they can be too coupled (the control loops depend on each other) to be controlled by decentralized controllers. In these cases, use of decouplers can make the loops independent enough of each other so that decentralized control can be used.

If decentralized control is applied, the one loops ability to be robust against opening and closing other loops can be an important factor. If not satisfied, setting one controller to manual can destabilize the whole system. If this ability is not possible to obtain with decentralized control due to coupling, using decouplers is one solution. In addition, the control system should be able to be robust against input saturation in the process inputs.

In the process industry the controlled variables (process input) are often control valves and these are limited to the range $0\% - 100\%$ which are hard constraints that cannot be violated.

1.2 Project outline

In Chapter 1 the SIMC tuning rule will be presented, and the proposed robust settings is derived. The traditional decoupler named *ideal decoupler* is presented, as well as a simplification of it, named *simplified decoupler*. Next, the newer decoupler method named *inverted decoupler*, which is lesser discussed in literature, is presented. The one-way decoupler which is a partial inverted decoupler is also presented. Last, the effect of model error when designing decouplers is briefly discussed.

In Chapter 2, the robust settings are tested on an multivariable example with model error in an off-diagonal element. The different decouplers are tested and PI controllers are designed for these decouplers.

In Chapter 3, a model for a two-phase high pressure vessel is derived. First, SISO examples are studied and the robust settings are applied and compared to regular SIMC settings with $\tau_c = \theta$. Next, the multivariable system is studied and decentralized PI controllers are designed for the system. The robustness criteria are tested with decentralized control with robust settings and a one-way decoupler.

The robustness criteria used in this report are:

1. Robustness against parameter changes.
2. Robustness against multivariable interactions including opening and closing other loops.
3. Robustness against input saturation.

1.3 Abbreviations and nomenclature

List of abbreviations

MIMO	Multiple Input Multiple Output
MPC	Model Predictive Control
PI	Proportional Integral
PID	Proportional Integral Derivative
PRGA	Performance Relative Gain Array
RGA	Relative Gain Array
SIMC	Simple/Skogestad Internal Model Control
SISO	Single Input Single Output

Nomenclature

$y(t)$	Process output, measured variable
$u(t)$	Process input, manipulated variable
$c(t)$	Controller output
$g(s)$	Transfer function, SISO
$G(s)$	Transfer matrix, MIMO
$\tilde{G}(s)$	Model of the system $G(s)$
$D(s)$	Decoupler
$k(s)$	Controller, SISO
$K(s)$	Controller, MIMO
K_c	Controller gain
τ_I	Integral time in controller
$\lambda(s)$	relative gain
$\Lambda(s)$	RGA
$\Gamma(s)$	PRGA

Chapter 2

Theory

In this chapter the SIMC tuning rule for first order plus time delay processes, and for integrating plus time delay processes will be presented (Skogestad, 2003a). In Seborg et al. (2004) it is stated that the derivative (D) part of PID controllers is often omitted in process industry control. Therefore, the focus in this report will be PI controllers. Next, a modification of the SIMC tuning rule which includes the worst case expected scenario is presented. These robust settings will be somewhat slower for nominal operation, but will be robust against changes in the process. In the last part, different decoupling techniques are presented, including ideal decoupling, simple decoupling, inverted decoupling and one-way decoupling. Also, the effect of process model error is discussed.

2.1 The SIMC tuning rule and the half rule

2.1.1 The SIMC tuning rule

The proportional integral (PI) controller is given by

$$k(s) = K_c \frac{\tau_I s + 1}{\tau_I s} \tag{2.1}$$

where K_c is the controller gain and τ_I is the integral time. Although only two parameters, selecting good ones can be cumbersome and even impossible if no systematic method is used. There are several tuning rules where these parameters are determined by experiments or from a simple model of the system. Several examples are listed in Seborg et al. (2004). One of these tuning rules is the SIMC tuning rule (Skogestad, 2003a). It preforms well for step changes and disturbance rejection (e.g. Skogestad (2003a) and Seborg et al. (2004)). One of its advantages is its simplicity, with simple equations and only one tuning parameter τ_c. This parameter is the desired closed loop time constant where the closed loop desired transfer function from reference

to output is

$$\left(\frac{y}{r}\right)_{\text{desired}} = \frac{1}{\tau_c s + 1} e^{-\theta s}$$

where θ is the time delay in the system. For the first order process with time delay

$$g(s) = \frac{k}{\tau_1 s + 1} e^{-\theta s}$$

the SIMC-PI settings are (Skogestad, 2003a)

$$K_c = \frac{1}{k} \frac{\tau_1}{\tau_c + \theta} = \frac{1}{k'} \frac{1}{\tau_c + \theta}; \qquad \tau_I = \min\{\tau_1, 4(\tau_c + \theta)\} \tag{2.2}$$

and the for the integrating process with time delay

$$g(s) = \frac{k'}{s} e^{-\theta s}$$

the SIMC-PI settings are

$$K_c = \frac{1}{k'} \frac{1}{\tau_c + \theta}; \qquad \tau_I = 4(\tau_c + \theta) \tag{2.3}$$

The tuning parameter τ_c is the desired closed-loop time constant. The SIMC-rule for fast response with good robustness is

$$\tau_c = \theta \tag{2.4}$$

2.1.2 The half rule

The *half rule* for model reduction is also presented in Skogestad (2003a). The original model is

$$\frac{\prod_j \left(-T_{j0}^{\text{inv}} s + 1\right)}{\prod_i \tau_{i0} s + 1} e^{-\theta_0 s}$$

with $T_{j0}^{\text{inv}} > 0$ and with τ_{i0} ordered according to magnitude, i.e. τ_{10} is the largest. To reduce the model to $e^{-\theta s}/(\tau_1 s + 1)$, the following approximations are used

$$\tau_1 = \tau_{10} + \frac{\tau_{20}}{2}; \qquad \theta = \theta_0 + \frac{\tau_{20}}{2} + \sum_{i \geq 3} \tau_{i0} + \sum_j T_{j0}^{\text{inv}} \tag{2.5}$$

If there are positive numerator time constant T_0, the cancellation of the numerator term $(T_0 s + 1)$ with the denominator term $(\tau_0 s + 1)$ is approximated by

$$\frac{T_0 s + 1}{\tau_0 s + 1} \approx \begin{cases} T_0/\tau_0 & \text{for } T_0 \geq \tau_0 \geq \theta \\ T_0/\theta & \text{for } T_0 \geq \theta \geq \tau_0 \\ 1 & \text{for } \theta \geq T_0 \geq \tau_0 \\ T_0/\tau_0 & \text{for } \tau_0 \geq T_0 \geq 5\theta \\ \frac{\tilde{\tau}_0/\tau_0}{(\tilde{\tau}_0 - \tau_0)s + 1} & \text{for } \tilde{\tau}_0 := \min(\tau_0, 5\theta) \geq T_0 \end{cases} \tag{2.6}$$

2.2 Robust SIMC settings

In Skogestad (2003a) it is suggested to use $\tau_c = \theta$ for robust controller settings with fast response. As will be demonstrated in this report, this can still give a too aggressive controller. Even though the model is quite good, e.g. as with the pressure dynamics in the tank in Section 4.1, the parameters in the model can vary quite much due to change in operational parameters, e.g. flow, level and pressure. If the process changes so that the controller becomes too aggressive, one solution is to detune the controller by increasing τ_c. The problem is that an increase in τ_c can make the response unnecessary slow. In this section, a method for selecting τ_c is proposed. The motivation for the proposed rules is to derive good robust settings without trial and error tuning on τ_c and which gives a satisfactory response for both nominal and worst case. The settings are based on the principle of detuning for increased robustness.

Robust settings:

1. Find k'_{wc} and θ_{wc}.
2. Select $\tau_{c,\,\text{wc}}$, e.g. $\tau_{c,\,\text{wc}} = 0$. Lower bound $\tau_{c,\,\text{wc}} > -\theta_{\text{wc}}$.
3. Calculate
$$\tau_{c,\,\text{nom}} = \frac{k'_{\text{wc}}}{k'_{\text{nom}}}\left(\tau_{c,\,\text{wc}} + \theta_{\text{wc}}\right) - \theta_{\text{nom}}$$
4. Calculate $\tau_c = \max(\tau_{c,\,\text{nom}}, \theta_{\text{nom}})$.
5. Calculate K_c and τ_I according to normal rule
$$K_c = \frac{1}{k'_{\text{nom}}}\frac{1}{\tau_c + \theta_{\text{nom}}}$$
$$\tau_I = \min(\tau_{1,\,\text{nom}}, 4(\tau_c + \theta_{\text{nom}}))$$

Where 'wc' is short for 'worst case' and 'nom' is short for 'nominal'. In the following, each step will be explained in more detail.

Step 1 For the integrating process

$$k'_{\text{wc}} = k'_{\text{max}}$$

and for the first order plus time delay process

$$k'_{\text{wc}} = \frac{k'_{\text{max}}}{\tau_{1,\,\text{min}}}$$

This is the maximum expected gain for the processes. By finding this gain, in addition to obtaining θ_{wc}, a controller can be based on the

worst case scenario which is expected to occur during normal operation.

Step 2 The SIMC-rule $\tau_c = \theta$ for fast, yet robust response need not necessary be used for the worst case. In fact, for a positive non-zero controller gain the lower bound is $\tau_c > -\theta$ (Skogestad, 2003a). With $\tau_c = 0$ the M_S value is 3.13 (see Appendix A.1 for definition of M_S) for the first order plus time delay process with $\tau_1 \leq 4(\tau_c + \theta)$ and 4.14 for the integrating plus time delay process, see Table A.1. This is higher than the guidelines of typical M_S values in the range of $1.2 - 2.0$ (see Appendix A.1), but these values applies for the worst case scenario. For these values, the lower bound on the gain margin is 1.47 and 1.29, respectively. Thus $\tau_{c,\,\mathrm{wc}} = 0$ may be too small for the integrating plus time delay process.

Step 3 The gain $K_{c,\,\mathrm{nom}}$ is selected equal to the gain $K_{c,\,\mathrm{wc}}$ for the worst case. To find the controller gain which gives $K_{c,\,\mathrm{nom}} = K_{c,\,\mathrm{wc}}$ the equation

$$\frac{1}{k'_{\mathrm{nom}}} \frac{1}{\tau_{c,\,\mathrm{nom}} + \theta_{\mathrm{nom}}} = \frac{1}{k'_{\mathrm{wc}}} \frac{1}{\tau_{c,\,\mathrm{wc}} + \theta_{\mathrm{wc}}}$$

is solved for $\tau_{c,\,\mathrm{nom}}$.

Step 4 If the value for $\tau_{c,\,\mathrm{nom}}$ found in Step 3 is smaller than θ_{nom}, it needs to be be increased to prevent the response to be too aggressive in the nominal case. Thus $\tau_c \geq \theta_{\mathrm{nom}}$ is set as a lower bound. Note that there is also an upper limit on τ_c. Finding the upper limit is discussed in Skogestad (2006).

Steps 5 The previous steps finds a tuning parameter $\tau_c \geq \theta_{\mathrm{nom}}$, and this is used in the normal SIMC-rule.

These settings will be tested on different cases throughout of the report.

2.3 Decentralized control

With decentralized control of the square multivariable process $G(s)$, shown in Figure 2.1, the controller $K(s)$ is used where each output only is paired

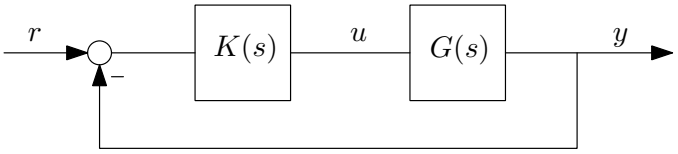

Figure 2.1: One degree of freedom control system.

with one input. In case of pairing on the diagonal of $G(s)$ the controller is

$$K(s) = \begin{bmatrix} k_1(s) & & & \\ & k_2(s) & & \\ & & \ddots & \\ & & & k_m(s) \end{bmatrix} \tag{2.7}$$

When the process is close to diagonal, i.e. the diagonal elements are dominate compare to the off-diagonal elements, one can design the controller elements $k_i(s)$ as if each diagonal element $g_{ii}(s)$ in $G(s)$ was a separate process.

If the process is coupled, it may not be apparent which input-output pair which should be paired. A tool which can be used to select the correct pairing is the *relative gain array* (RGA). The *relative gain* (Bristol, 1966) between the isolated (open) loop ($g_{ij}(s)$) and the same loop with all other control loops closed ($\hat{g}_{ij}(s)$) is defined as

$$\lambda_{ij}(s) = \frac{g_{ij}(s)}{\hat{g}_{ij}(s)} \tag{2.8}$$

The relative gain array (e.g. Skogestad and Postlethwaite (2005)) then becomes

$$\Lambda(s) = G(s) \times G^{-T}(s) \tag{2.9}$$

where '$\times$' is element-by-element multiplication. In order to select a good paring, Skogestad and Postlethwaite (2005) recommends pairing on elements which is close to identity at frequencies around closed-loop bandwidth and to avoid pairing on negative steady-state relative gains. The RGA gives a good indication on two-way interaction, but it is not possible to measure if the interaction goes one or both ways. A tool for measuring one-way interactions is the *performance relative gain array* (PRGA). It is defined as (Skogestad and Postlethwaite, 2005)

$$\Gamma(s) = G_{\text{diag}}(s)G^{-1}(s) \tag{2.10}$$

where $G_{\text{diag}}(s) = \text{diag}\{g_{ii}(s)\}$ is the diagonal elements of $G(s)$. While the elements in RGA are scaled, the elements in PRGA depends on relative scaling of the outputs.

In order to take other loops in and out of service, the controllers need to be designed independently (Skogestad and Postlethwaite, 2005). With the *independent design method* each loop of $G(s)$ is designed to be stable, but the controllers may be tuned to handle interactions between the loops, i.e. making some loops faster than the others.

2.4 Decoupling of multivariable systems

In recent years, it has been a large focus on model predictive control for controlling multivariable systems (Maciejowski, 2002). Its advantage is that the control is optimal with respect to a defined objective function and thus performance is expected to be noticeable better than with decentralized control. One other aspect with model predictive control which is just as important, is the handling of constraints, whereas a simple decentralized controller structure will act as open loop when the inputs saturates.

The disadvantage with model predictive control is the need for implementation of an advanced system which needs to continuous (or regularly) do numerical optimization. For smaller, yet coupled systems it may not be economical to develop a model and install the advanced controller. For these systems, techniques as decoupling may be a simple, yet good way to maintain stability and reduce the effect of input saturation.

In this section, the three different decoupling techniques presented in Wade (1997) will be described. Also, a one-way decoupler which can be seen as a feed-forward element will be described. Decoupling can be extended to an $n \times n$ system, but are rarely used for systems with $n > 3$ because of increase in complexity (Seborg et al., 2004). Thus, the discussion in this report will be limited to the 2×2 system

$$\begin{aligned} y_1 &= G_{11}u_1 + G_{12}u_2 \\ y_2 &= G_{21}u_1 + G_{22}u_2 \end{aligned} \tag{2.11}$$

where G_{ij} are known process transfer functions, y_i are process outputs and u_j are the actual process inputs. The decoupler from the controller output c_k to the process input u_j is

$$\begin{aligned} u_1 &= D_{11}c_1 + D_{12}c_2 \\ u_2 &= D_{21}c_1 + D_{22}c_2 \end{aligned} \tag{2.12}$$

Ideally the decoupler removes all off-diagonal elements, giving

$$y = GDc = G_{diag}c \tag{2.13}$$

where G_{diag} contains only the diagonal elements of G. In other words, ideally the decoupler is given by

$$D = G^{-1}G_{diag} \tag{2.14}$$

Thus, decoupling is a technique similar to inverse controllers and its use is limited to systems which are not singular. In Skogestad and Postlethwaite (2005) it is stated that decouplers or other inverse-based controllers should not be used for systems with large RGA elements. When choosing a decoupler technique, Shinskey (1996) argues that decouplers should be as simple as possible and reflect process relationships rather than abstract mathematical relationships.

2.4.1 Ideal decoupling

With *ideal decoupling* (shown in Figure 2.2), the objective is to completely decouple the off-diagonal elements so that the apparent process is

$$\begin{aligned} y_1 &= G_{11}c_1 \\ y_2 &= G_{22}c_2 \end{aligned} \tag{2.15}$$

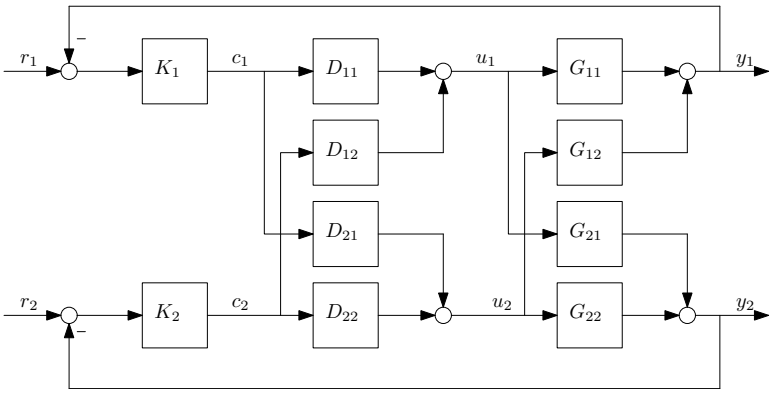

Figure 2.2: Ideal decoupling.

Combining (2.11), (2.12) and (2.15) it can be shown that the decoupler elements D_{ij} are

$$\begin{aligned} D_{11} &= \frac{G_{11}G_{22}}{G_{11}G_{22} - G_{12}G_{21}} \\ D_{12} &= \frac{-G_{12}G_{22}}{G_{11}G_{22} - G_{12}G_{21}} \\ D_{21} &= \frac{-G_{11}G_{21}}{G_{11}G_{22} - G_{12}G_{21}} \\ D_{22} &= \frac{G_{11}G_{22}}{G_{11}G_{22} - G_{12}G_{21}} \end{aligned} \tag{2.16}$$

The decoupler elements are relatively complex, but the apparent process (decoupler and process viewed as a whole) becomes diagonal with only the diagonal elements of the process G on the diagonal.

2.4.2 Simplified decoupling

The *simplified decoupler* (shown in Figure 2.3) is given in Morari and Zafiriou (1989) as

$$D = G^{-1}((G^{-1})_{\text{diag}})^{-1} \tag{2.17}$$

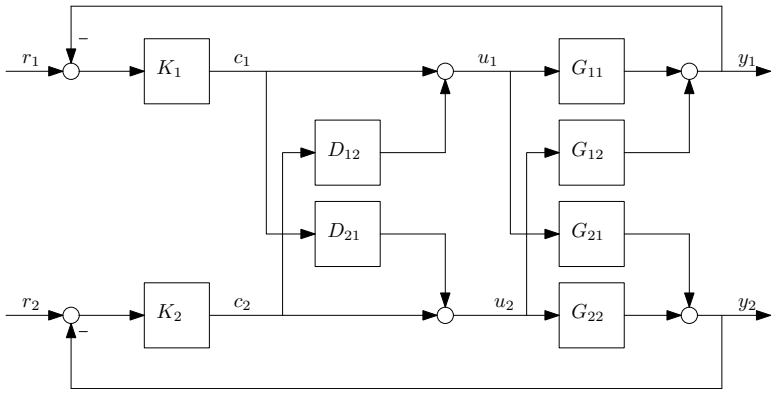

Figure 2.3: Simplified decoupling.

This decoupler is a modification of the ideal decoupler where $D_{11} = D_{22} = 1$ which gives the simpler decoupler elements

$$\begin{aligned} D_{12} &= -\frac{G_{12}}{G_{11}} \\ D_{21} &= -\frac{G_{21}}{G_{22}} \end{aligned} \tag{2.18}$$

Now the apparent process is changed to the more complex form

$$\begin{aligned} y_1 &= \frac{G_{11}G_{22} - G_{12}G_{21}}{G_{22}} c_1 \\ y_2 &= \frac{G_{11}G_{22} - G_{12}G_{21}}{G_{11}} c_2 \end{aligned} \tag{2.19}$$

With this decoupler, the objective to decouple the off-diagonal elements is fulfilled, but the apparent process is changed. Hence the controllers needs to be retuned after installation. Also the apparent process can be difficult to understand based on a physical interpretation.

2.4.3 Inverted decoupler

In Gagnon et al. (1998) is is shown that the ideal decoupler (2.12) with elements given by (2.16) can be simplified to

$$\begin{aligned} u_1 &= c_1 - \frac{G_{12}}{G_{11}} u_2 \\ u_2 &= c_2 - \frac{G_{21}}{G_{22}} u_1 \end{aligned} \tag{2.20}$$

which gives the same decoupling elements as the simplified decoupler, but the same apparent process as the ideal decoupler, giving it the same advantages as mentioned in Section 2.4.1. This decoupler is called the *inverted*

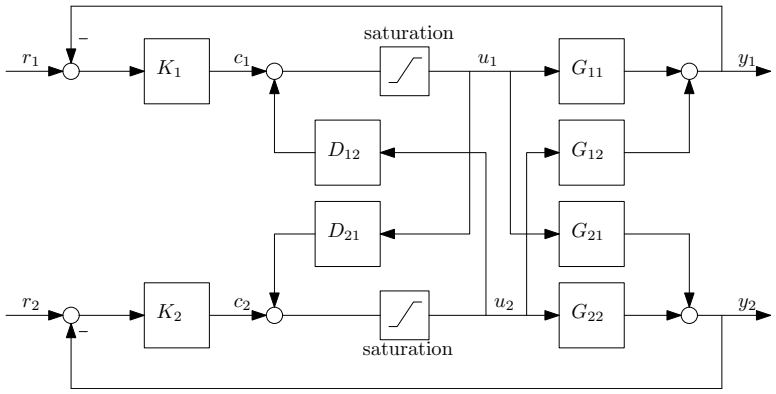

Figure 2.4: Inverted decoupling.

decoupler and is shown in Figure 2.4, where the input saturation is included to show that the actual process input is measured.

Studying Figure 2.4 it is apparent that with inverted decoupling the input to one process input (u_i) can be viewed as a disturbance to the other controllers output (c_k). One advantage of this decoupler is that the actual process input is measured, so the effect of actuator saturation is counteracted with the decoupler.

In Wade (1997), three important advantages with inverted decoupling are listed:

1. *The apparent process seen by each controller when [inverted] decoupling is implemented is the same as if there were no decoupling and the alternate controller were in manual mode.*

2. *Each decoupled control loop is immune to abnormalities (e.g. valve at a limit or a secondary controller in manual) in the secondary of the opposite control loop.*

3. *Inverted decoupling can often be implemented with in a DCS (Distributed Control System) using a PID function block with feedforward input.*

Gagnon et al. (1998) also discusses the disadvantage of inverted decoupling over the other two techniques to be that implementation with lead-lag and delay function block may decrease performance. Even so, the robustness of inverted decoupling with respect to opening and closing other loops, as well as robustness with respect to input saturation, makes it the most promising of the presented decouplers.

2.4.4 One-way decoupling

Often, the coupling is not as strong both ways in the process. In these cases, only decoupling of the strongest off-diagonal element(s) can yield a significant improvement over a pure decentralized controller structure. Use of feedforward to reduce coupling from the j^{th} loop to the i^{th} loop can be seen as a partly decoupler. In fact, the inverted decoupler with only decoupling one way will be the same as the kind of feedforward control described in Shinskey (1996). In addition to be simpler, the destabilization which can result from using decoupling is eliminated with partial decoupling (Shinskey, 1996). This is a very important property, which will be studied further in Section 3.5. Also, one-way decouplers are generally much less sensitive to input uncertainty (Morari and Zafiriou, 1989).

If one-way decoupling is used from u_1 to c_2, (2.20) is reduced to

$$\begin{aligned} u_1 &= c_1 \\ u_2 &= c_2 - \frac{G_{21}}{G_{22}} c_1 \end{aligned} \tag{2.21}$$

This gives the apparent process

$$\begin{aligned} y_1 &= \left(G_{11} - G_{12} \frac{G_{21}}{G_{22}} \right) c_1 + G_{12} c_2 = \frac{G_{11}}{\lambda_{11}} c_1 + G_{12} c_2 \\ y_2 &= G_{22} c_2 \end{aligned} \tag{2.22}$$

where λ_{11} is the relative gain. This decoupling is the same as removing D_{12} in Figure 2.4.

2.4.5 Decoupling with process model error

As mentioned earlier, one problem of using decoupling is that it includes the inverse of the process. When the model of the process ($\tilde{G}$) differs from the real plant (G) the apparent process $y = PDc$ is no longer given by (2.15) for the ideal and inverted decouplers. With $D = \tilde{G}^{-1}\tilde{G}_{\text{diag}}$ the apparent process becomes

$$GD = G\tilde{G}^{-1}\tilde{G}_{\text{diag}} \tag{2.23}$$

and for the 2×2 system this is

$$\begin{aligned} GD = &\frac{1}{\tilde{G}_{11}\tilde{G}_{22} - \tilde{G}_{12}\tilde{G}_{21}} \\ &\cdot \begin{bmatrix} \tilde{G}_{11}(G_{11}\tilde{G}_{22} - G_{12}\tilde{G}_{21}) & \tilde{G}_{22}(G_{12}\tilde{G}_{11} - G_{11}\tilde{G}_{12}) \\ \tilde{G}_{11}(G_{21}\tilde{G}_{22} - G_{22}\tilde{G}_{21}) & \tilde{G}_{22}(G_{22}\tilde{G}_{11} - G_{21}\tilde{G}_{22}) \end{bmatrix} \end{aligned} \tag{2.24}$$

Note that if $\tilde{G} = G$, (2.24) is reduced to (2.15). For the simplified decoupler,

using $D = \tilde{G}^{-1}((\tilde{G}^{-1})_{\text{diag}})^{-1}$, the apparent process $y = GDc$ becomes

$$GD = G\tilde{G}^{-1}((\tilde{G}^{-1})_{\text{diag}})^{-1} \tag{2.25}$$

so also in this case, the inverse of the model ($\tilde{G}^{-1}$) has an effect of the sensitivity to model errors.

Chapter 3

A two-way interactive process

In this chapter, a simple 2×2 interactive process will be studied. The process is purely a theoretical example, and is a modified example from Skogestad and Postlethwaite (2005). The process is the linear time-invariant system

$$G(s) = \frac{1}{s+1}\begin{bmatrix}1 & g_{12}\\ 5 & 1\end{bmatrix} \tag{3.1}$$

with $g_{12} \in [0.17, -1]$. The purpose with this example is to look at how to obtain controllers which are good for all values of the uncertain element g_{12}, and which are as little as possible dependent of the other loops. For convenience, the study will be limited to the three cases $g_{12} = \{0.17, -0.2, -1\}$. Further, all simulations are done with a time-delay θ of 0.5 s. In this way the upper achievable controller gains are limited. The controllers tested are simple PI controllers in addition to decouplers.

3.1 Decentralized control

In order to select the best pairing of the input and outputs, the steady-state RGA is calculated for the three different cases

$$\begin{aligned}\Lambda_1(0) &= \begin{bmatrix}6.67 & -5.67\\ -5.67 & 6.67\end{bmatrix}; \quad \Lambda_2(0) = \begin{bmatrix}0.5 & 0.5\\ 0.5 & 0.5\end{bmatrix}\\ \Lambda_3(0) &= \begin{bmatrix}0.167 & 0.833\\ 0.833 & 0.167\end{bmatrix}\end{aligned} \tag{3.2}$$

There is no loss in generality of using the steady-state RGA in this case, since the RGA (for this particular example) is the same for all frequencies. From a first inspection of the different RGA matrices, it is evident that this process is difficult to control with one paring and one set of controllers. In order

not to pair on negative steady-state elements of the RGA (as mentioned in Section 2.3), Λ_1 shows that pairing on the off-diagonal elements should be avoided. At the same time, with $g_{12} = -1$ it can be seen from Λ_3 that it is recommended to pair on the off-diagonal elements because these are closest to identity.

With pairing on the diagonal, and using independent design of the diagonal elements in $G(s)$, the SIMC controller gain parameters will be

$$K_{c1} = \frac{1}{k_1}\frac{\tau_1}{\tau_c + \theta} = \frac{1}{\tau_{c1} + 0.5} \qquad K_{c2} = \frac{1}{\tau_{c2} + 0.5}$$

Because of the large off-diagonal element $G_{21}(s)$, using $\tau_c = \theta$ for the two loops gives a unsatisfactory control. As discussed in Skogestad and Postlethwaite (2005) the PRGA can be used to indicate which of the loops should be fastest. A large element in a row of the PRGA indicates that fast control is needed. The steady-state PRGA for the three cases is

$$\begin{aligned} \Gamma_1(0) &= \begin{bmatrix} 6.67 & -1.13 \\ -33.3 & 6.67 \end{bmatrix}; \quad \Gamma_2(0) = \begin{bmatrix} 0.50 & 0.10 \\ -2.50 & 0.50 \end{bmatrix} \\ \Gamma_3(0) &= \begin{bmatrix} 0.167 & 0.167 \\ -0.833 & 0.167 \end{bmatrix} \end{aligned} \tag{3.3}$$

For all cases, the second row in Γ is large and the magnitude of $\frac{\gamma_{21}}{\gamma_{22}}$ is 5 (due to $\Gamma_i = G^{-1}$ since $\tilde{G} = I$). Thus, we must control y_2 faster than y_1. Since the independent design strategy is followed, $k_2(s)$ is designed based on $G_{22}(s)$ and thus $\tau_{c2} = \theta$ is used. This gives

$$K_{c2} = 1 \qquad \tau_{I2} = \min\{\tau_2, 4(\tau_{c2} + \theta)\} = \tau_2 = 1$$

If y_2 is perfectly controlled, closing y_1 will give $y_1 = \hat{g}_{11}u_1 = \frac{g_{11}}{\lambda_{11}}u_1$. If the RGA element is between 0 and 1, it means that the gain will increase when closing the loop. For these cases, if the open-loop gain $k_1' = \frac{k_1}{\tau_1}$ is scaled with $|\lambda_{ii}|$ around the crossover frequency the actual gain when closing the loop will be found. The different cases of g_{12} gives $\lambda_{11} = \{6.67, 0.5, 0.167\}$, so selecting the worst case of 0.167, the worst case $\hat{k}_1'$ will be $\hat{k}'_{1,\,\text{worst case}} = 1/0.167 = 6$ where $\hat{k}_1' = \frac{k_1'}{\lambda_{11}}$. With $\hat{k}'_{1,\,\text{nom}} = 1/0.5 = 2$ the tuning parameter is found to be $\tau_{c1} = 14\theta$ using

$$\begin{aligned} \tau_{c,\,\text{nom}} &= \frac{\hat{k}'_{1\,\text{wc}}}{\hat{k}'_{1\,\text{nom}}}(\tau_{c,\,\text{wc}} + \theta_{\text{wc}}) - \theta_{\text{nom}} = \frac{6}{2}(4\theta + \theta) - \theta = 14\theta \\ \tau_c &= \max(\tau_{c,\,\text{nom}}, \theta_{\text{nom}}) = \max(14\theta, \theta) = 14\theta \end{aligned}$$

This gives the controller

$$\begin{aligned} K_{c1} &= \frac{1}{\hat{k}'_{1\,\text{nom}}}\frac{\tau_1}{\tau_c + \theta} = \frac{1}{2}\frac{1}{14 \cdot 0.5 + 0.5} = 0.067 \\ \tau_{I1} &= \min\{\tau_1, 4(\tau_{c1} + \theta)\} = \tau_1 = 1 \end{aligned}$$

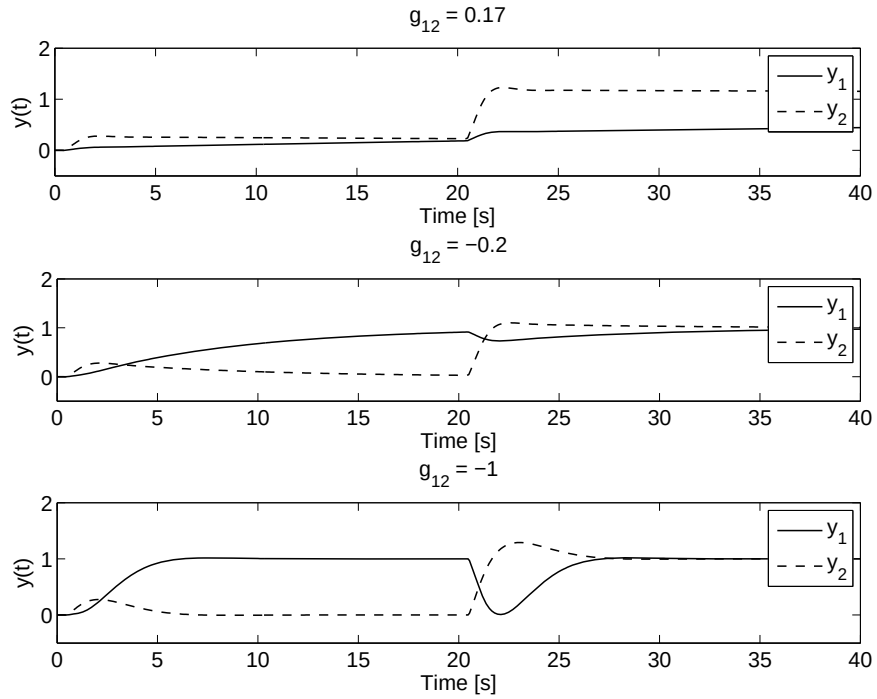

Figure 3.1: Decentralized control with diagonal pairing.

where $\hat{k}_1 = \frac{k_1}{\lambda_{11}}$.

The responses to a unit step in both loops are shown in Figure 3.1. As expected, y_2 has a fast response with small overshoot. In order to get a stable response for all cases for y_1, the controller needed to be detuned noticeably, as can be seen from the very slow response for $g_{12} = 0.17$. This is as expected, since the relative gain λ_{ii} varies with a factor of 40 between the extremes of g_{12}.

3.2 Ideal and inverted decoupling

Many of the problems arising when using decentralized control of the process (3.1) is due to the large element $G_{21}(0) = 5$. One way of minimizing the effect of this off-diagonal element is to use a decoupler. The problem when designing the decoupler is that the overall process only will be completely decoupled for the nominal case. When there is a model error in the decoupler, this will affect both the off-diagonal elements in the overall process as well as the diagonal. This can be seen from (2.24) where the off-diagonal elements in general are non-zero for $\tilde{G} \neq G$. In addition, the decoupler should not be designed based on a model with large RGA elements. Thus, designing the decoupler based on $g_{12} = 0.17$ is not recommended since it

will make it sensitive to model error. For the decouplers, the model

$$\tilde{G}(s) = \frac{1}{s+1}\begin{bmatrix} 1 & -0.4 \\ 5 & 1 \end{bmatrix} \tag{3.4}$$

will be used. The gain of the unknown element is selected to be $\tilde{g}_{12} = -0.4$ based on the range $g_{12} \in [-1, 0.17]$. For the ideal decoupler, using (2.16) gives the decoupler elements

$$\begin{aligned} D_{11} &= 0.33 \\ D_{12} &= 0.13 \\ D_{21} &= -1.67 \\ D_{22} &= 0.33 \end{aligned} \tag{3.5}$$

and using (2.18), the decoupler elements for the inverted decoupler is

$$\begin{aligned} D_{12} &= 0.4 \\ D_{21} &= -5 \end{aligned} \tag{3.6}$$

For the nominal case ($g_{12} = -0.4$), the decoupled system will be completely coupled ($\Lambda = I$) if the decoupler is realizable. Hence, the controllers are designed based on the diagonal elements of $\tilde{G}$, but at the same time the effect of model error must be taken into account. For the three different cases of g_{12}, the decoupled system GD using (2.23) is

$$\begin{aligned} GD &= \frac{1}{s+1}\begin{bmatrix} 0.05 & 0.19 \\ 0 & 1 \end{bmatrix}; \quad GD = \frac{1}{s+1}\begin{bmatrix} 0.67 & 0.07 \\ 0 & 1 \end{bmatrix} \\ GD &= \frac{1}{s+1}\begin{bmatrix} 2 & -0.2 \\ 0 & 1 \end{bmatrix} \end{aligned} \tag{3.7}$$

The element $(GD)_{22}$ stays constant, but $(GD)_{11}$ varies quite a lot. To design a robust PI controller for this process, the procedure Section in 2.2 is followed. With $k'_{1,\,\text{worst case}} = 2$, $k'_{1,\,\text{nom}} = 0.67$ and $\theta = 0.5$ for both nominal and worst case, selecting $\tau_{c1,\text{worst case}} = 0$, gives the value $\tau_{c1} = 2\theta$. This gives the controller

$$\begin{aligned} K_{c1} &= \frac{1}{k'_{1,\,\text{nom}}}\frac{1}{\tau_{c1}+\theta} = \frac{1}{1}\frac{1}{2\cdot 0.5 + 0.5} = 0.67 \\ \tau_{I1} &= \min\{\tau_1, 4(\tau_{c1}+\theta)\} = \tau_1 = 1 \end{aligned}$$

With $\tau_{c2} = \theta$ (the same controller as with decentralized control) the response for ideal and inverted decoupling is shown in Figure 3.2, where it can be seen from the lower plot that even a lower value for $\tau_{c1,\text{wc}}$ may be used. Overall, the effect of decoupling is evident when comparing Figures 3.1 and 3.2. The response of y_1 is faster, and the effect of coupling is much smaller. Note that the decoupling is not complete due to use of the same decoupler for all the cases. This is because of the problem with model error as discussed above.

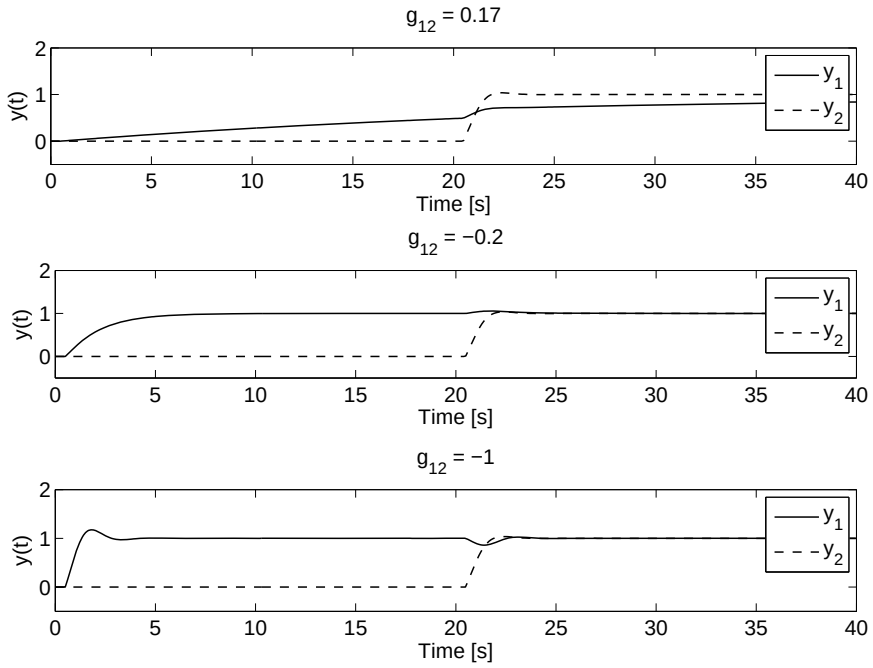

Figure 3.2: Ideal, simplified and inverted decoupling without saturation.

3.3 Simplified decoupling

As described in Section 2.4.2, simplified decoupling changes the apparent process, even in the nominal case. The decoupler elements are the same as with the inverted decoupler (3.6). Therefore, in order to tune the controllers it is necessary to calculate the apparent process also in the nominal case. Using (2.25), GD is calculated in the same manner as in the previous section to be

$$\begin{aligned} GD &= \frac{1}{s+1}\begin{bmatrix} 0.15 & 0.57 \\ 0 & 3 \end{bmatrix}; \quad GD = \frac{1}{s+1}\begin{bmatrix} 2 & 0.20 \\ 0 & 3 \end{bmatrix} \\ GD &= \frac{1}{s+1}\begin{bmatrix} 6 & -0.6 \\ 0 & 3 \end{bmatrix} \end{aligned} \tag{3.8}$$

By comparing (3.7) with (3.8), the difference is found to be a gain-increase of 3 in the latter. Therefore, the same controllers will be used as with ideal and simplified decoupling, but with a gain-increase of 3. The response is as expected identical with ideal and simplified decoupling and is shown in Figure 3.2. The disadvantage with simplified decoupling becomes more clear with this example, since the diagonal elements in the overall system GD is changed. With a physical example, this means that the whole process will in fact change, and that the physical understanding of the loops will easily be lost.

3.4 The effect of opening and closing loops

In addition to have controllers which are robust with respect to changes in the process, it is also in many applications important to have a control system which remains stable if loops are taken out of service. By using an independent design method when designing the decentralized controllers, this property is tried to be maintained. When using the decouplers, the response was identical for all three decouplers when both loops were in operation without any saturation. In this section, the effect of opening the loops will be studied.

When loop 1 is taken out of service ($c_1 = 0$ where c_1 is the output from the controller), both decentralized control and the decouplers manage to control y_2 more or less unaffected. In fact, the response for y_2 is more or less identical for decentralized control and decoupling. This can be explained by the fact that the effect of the large element $G_{21}(s)$ is limited or removed when $c_1 = 0$. When the output of the controller is non-zero but constant, this will not be the case. This will happen when the controller goes into saturation, which will be addressed in the next section.

With $c_2 = 0$, the decentralized controllers looses control of loop y_1 as can be seen in Figure 3.3. From Figure 3.4 it can be seen that the three different decouplers manage to maintain control of y_1 without any difference in the response of y_2.

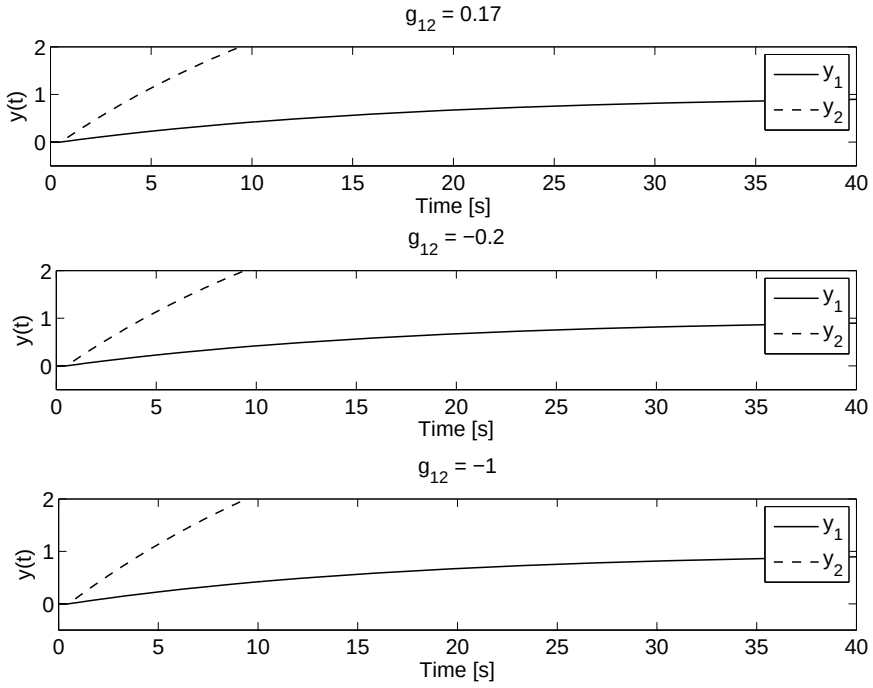

Figure 3.3: Decentralized control looses control with loop 2 open ($c_2 = 0$).

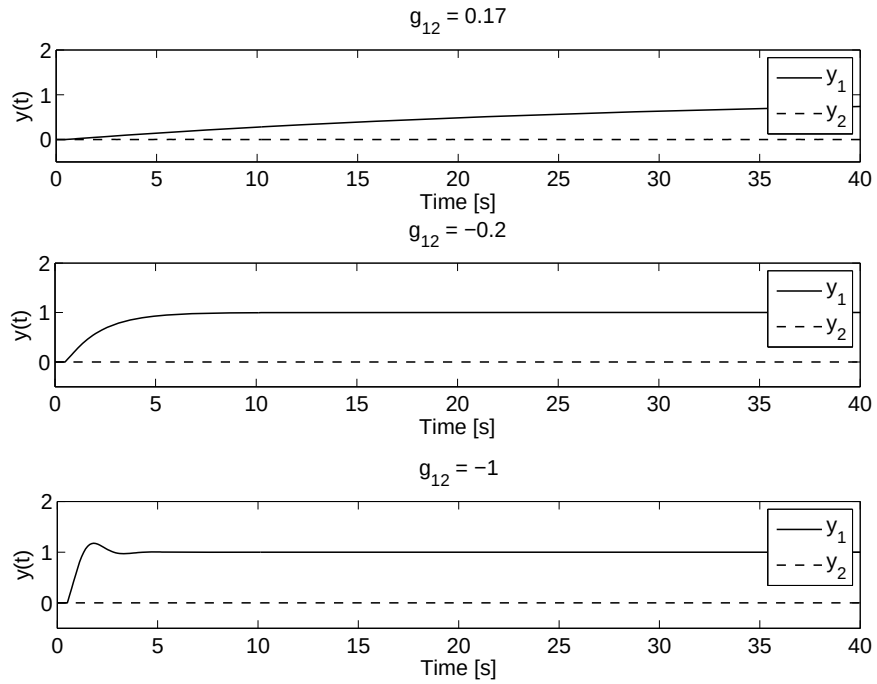

Figure 3.4: Ideal, simplified and inverted decoupling with loop 2 open ($c_2 = 0$).

3.5 The effect of input saturation

Until now, there have been no difference between the different decouplers. In this section, the effect of input saturation will be studied and the different decouplers will be compared. As opposed to the case with open loop, saturation in both loops will affect the response for the decouplers differently, but saturation in loop 1 is most illustrating and will be the focus of discussion in this section. With saturation

$$u_1 \in [0.2, 0.4]$$

and u_2 without saturation, the response for decentralized control is shown in Figure 3.5, the response for ideal and simplified decoupling is shown in Figure 3.6, and the response for inverted decouping is shown in Figure 3.7.

Comparing these three figures, the first observation is that ideal and simplified decoupling actually deteriorate the response compared to not using any decoupling. For all cases of g_{12} in Figure 3.6, y_2 is heavily influenced by saturation in u_1, and for the first case $g_{12} = 0.17$, the whole system becomes unstable. Inverted decoupling on the other hand, manages to control the system with saturation as can be seen in Figure 3.7. The response for y_2

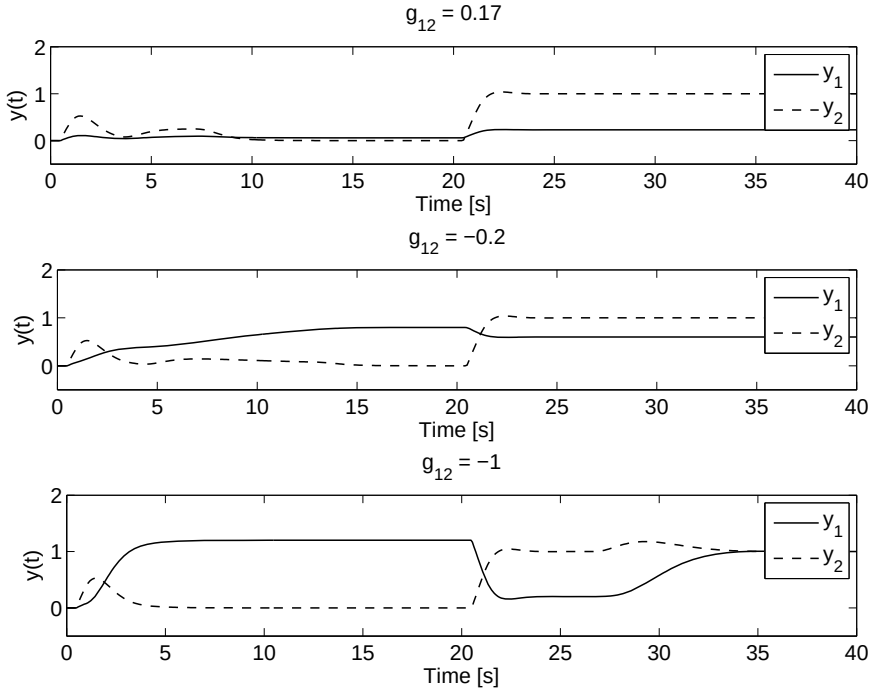

Figure 3.5: Decentralized control with u_1 saturated.

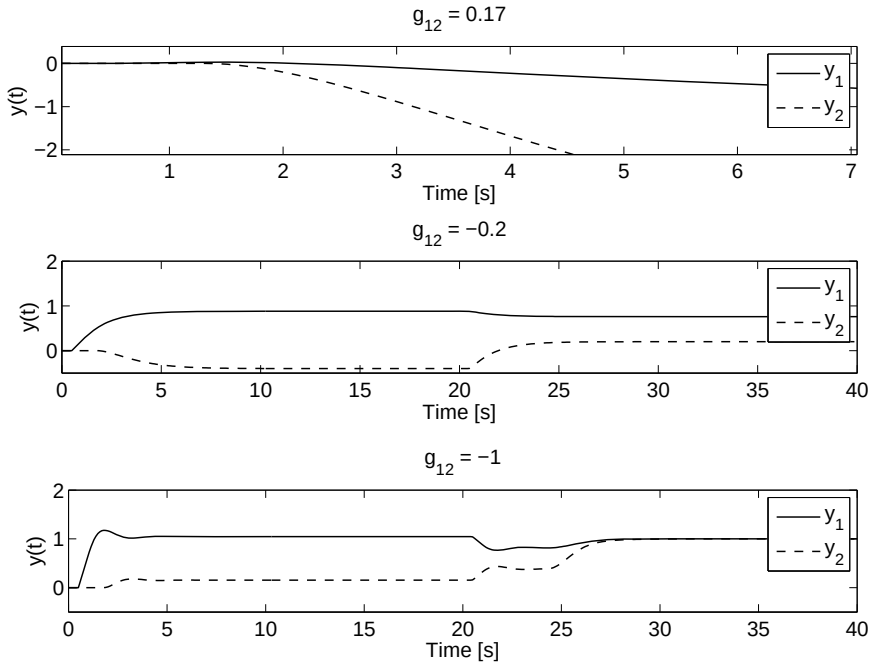

Figure 3.6: Ideal and simplified decoupling with u_1 saturated.

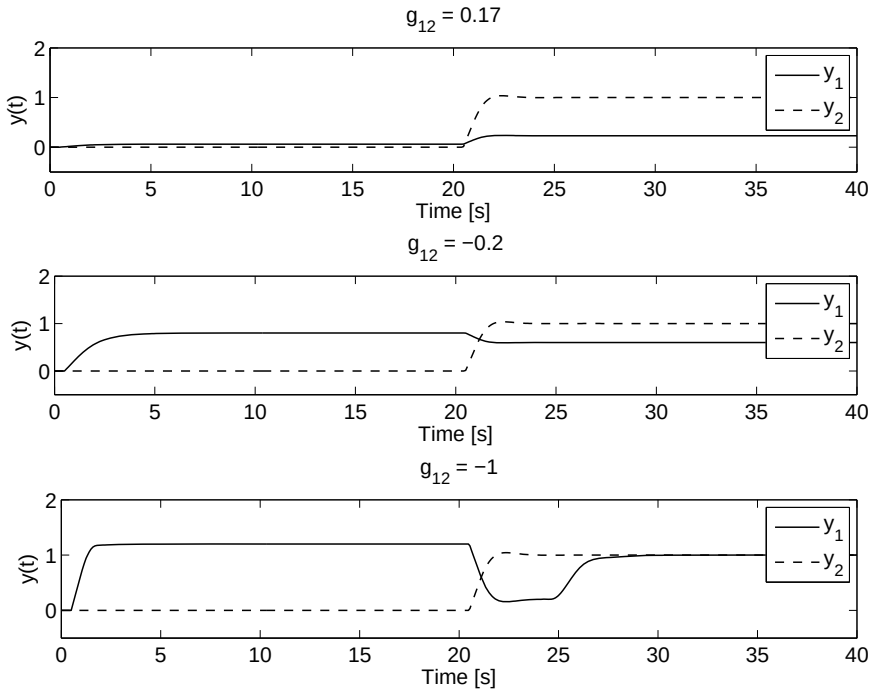

Figure 3.7: Inverted decoupling with u_1 saturated.

is unaffected by saturation in u_1 and the response is noticeably better than for decentralized control.

With the different cases tested in this chapter, inverted decoupling seems to be the best alternative when using decoupling. This is in accordance with the comparison of the different decouplers in Section 2.4. One important factor, which is the case for all decouplers, is to avoid using a process model which has large RGA elements.

3.6 One-way decoupling

As described in Section 2.4.4, one-way decoupling can give a good result when the coupling is stronger in one way than in the other. To design a controller for the one-way decoupled process, the apparent process (2.22) is used as starting point. In similar manner as in Section 3.1, $k_1(s)$ is designed based on λ_{11}, but the effect of decoupling must also be considered. Using (3.7) (the effect the one-way decoupler has on loop 1 is the same as the full decoupler), the worst case and nominal gains are

$$k'_{1,\,\mathrm{wc}} = \frac{k'_1}{\lambda_{11,\,\mathrm{wc}}}(GD)_{11,\,\mathrm{wc}} = \frac{1}{0.167}\cdot 2 = 12.0$$

$$k'_{1\,\mathrm{nom}} = \frac{k'_1}{\lambda_{11,\,\mathrm{nom}}}(GD)_{11,\,\mathrm{nom}} = \frac{1}{0.5}\cdot 0.67 = 1.34$$

Using the procedure from Section 2.2 with $\tau_{c1,\,\text{worst case}} = 0$, τ_{c1} is found to be

$$\tau_{c1} = 7.9\theta$$

This will give the robust settings

$$K_{c1} = \frac{1}{k'_{1\,\text{nom}}} \frac{\tau_1}{\tau_c + \theta} = \frac{1}{1.34} \frac{1}{7.9 \cdot 0.5 + 0.5} = 0.168$$
$$\tau_{I1} = \min\{\tau_1, 4(\tau_{c1} + \theta)\} = \tau_1 = 1$$

where $\hat{k}_1 = \frac{k_1}{\lambda_{11}}$. Loop 2 is nominally completely decoupled and $k_2(s)$ will be designed based on $G_{22}(s)$ with $\tau_{c2} = \theta$ which gives the same controller parameters as with decentralized control in Section 3.1.

In fact, using a one-way decoupler from u_1 to c_2 gives a result almost as good as inverted decoupling in the previous sections. The largest difference will be in the case when there is a saturation in u_2. This saturation is not counteracted since there are no decoupling from u_2 to c_1 ($D_{12} = 0$ in Figure 2.4). Using the saturation

$$u_2 \in [-1, -0.5]$$

and u_1 without saturation, a comparison of the effect of saturation in u_2 with inverted decoupling and one-way decoupling is shown in Figure 3.8. Only the case $g_{12} = -1$ is shown, since this is the case with most interactions. The effect of saturation in u_2 is, as expected, larger on y_1 with one-way decoupler than with inverted decoupler. Note that the reason for inverted decoupling not being perfect for y_1 is that the model of the process is different from the actual process, as discussed earlier. Even though the inverted decoupler is better with respect to y_1, the simplicity of the one-way decoupler makes it a good choice for this process.

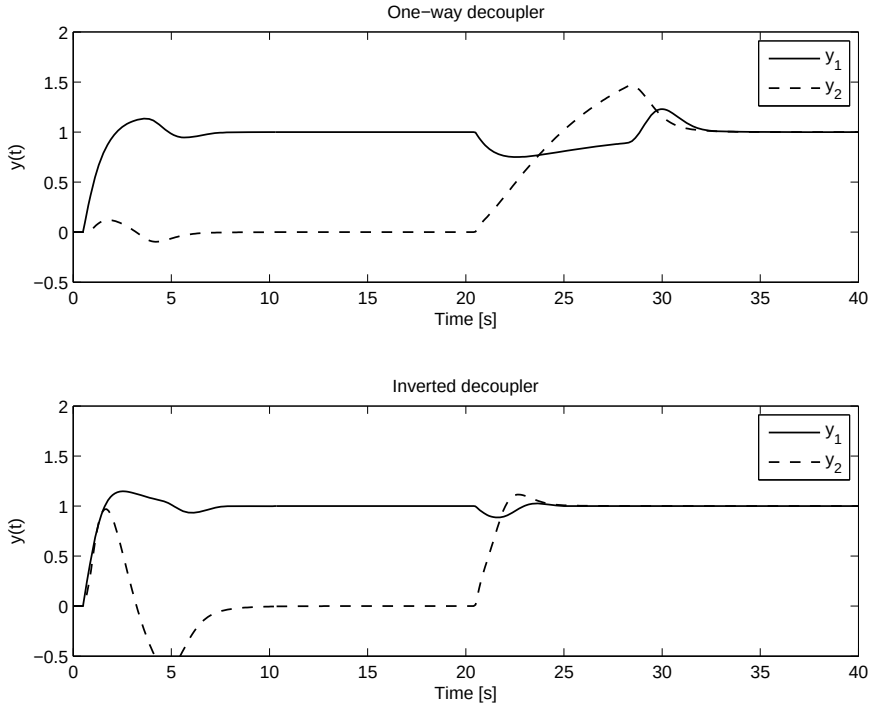

Figure 3.8: Comparison of inverted decoupling and one-way decoupling when u_2 is saturated and $g_{12} = -1$.

Chapter 4

A multivariable high pressure vessel

In the previous chapter, a simple illustrating multivariable example was used to study the different control structures. In this chapter, models based on physical examples will be studied. First-principle models will be derived and based on these, controller parameters will be calculated. The basis for the examples is the two-phase tank from Skogestad and Wolff (1991). The tank represents an oil-gas separator where a high-pressure two-phase well stream is separated into liquid and gas.

First, SISO systems where only one parameter has a dynamic effect will be studied, then the complete system will be studied. All the simulations will be done in Simulink, with the derived non-linear models implemented. The linearized models found are only used for analysis and controller design. When calculating the Laplace transform, the initial condition $x(t = 0)$ gives a contribution to the solution. For stable systems, this transient response will die out over time. Therefore, this part is omitted when deriving transfer functions, and the simulations are run long enough prior to defined start time in order to make this effect die out.

4.1 Modelling and control of pressure in gas tank

In this section, control of the pressure in the gas tank shown in Figure 4.1 will be studied. The in-flow q_{in} is not controlled and viewed as a disturbance. Even though the volume of the tank (V_{tank}) is constant, cases where the volume can change will be studied, while the dynamics will not be considered (only the steady-state effect of the liquid volume will be considered). The reason for a variable volume is because the liquid holdup in a multivariable tank will determine the volume $V = V_{\text{tank}} - V_L$ left for the gas. The temperature (T) is also a variable which can change during operation, but the temperature dynamics is assumed slow enough to be neglected. The pres-

sure inside the tank is assumed larger than the outflow pressure, $P > P_{\text{out}}$, and the outflow pressure (P_{out}) is assumed constant.

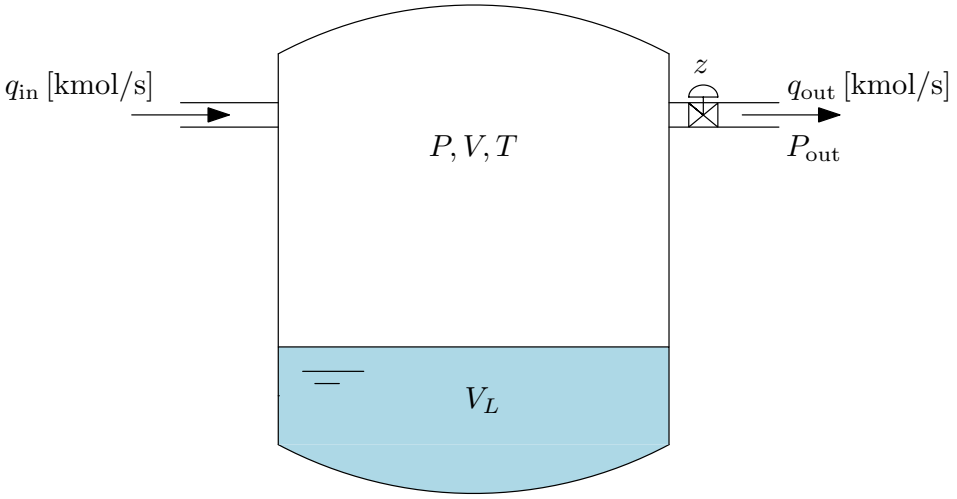

Figure 4.1: Tank with variable volume due to liquid in the bottom of the tank.

Assuming an ideal gas, ideal gas law (e.g. Skogestad (2003b))

$$PV = nRT \tag{4.1}$$

can be used to derive the material balance for the gas, where P [Pa] is pressure, n is moles of gas, $R = 8.3144\,[\frac{\text{J}}{\text{K}\cdot\text{mol}}]$ is the ideal gas constant and T [K] is the temperature of the gas. Differentiate (4.1) with respect to time gives

$$\dot{P}V + P\dot{V} = \dot{n}RT + nR\dot{T}$$

Temperature and volume dynamics are neglected, i.e. $\dot{T} = 0$ and $\dot{V} = 0$. Rearranging and using $\dot{n} = q_{\text{in}} - q_{\text{out}}$ [mol/s] gives

$$\frac{dP}{dt} = \frac{RT}{V}(q_{\text{in}} - q_{\text{out}}) \qquad [\text{Pa/s}] \tag{4.2}$$

The flow out of the valve can be represented by the equation (Skogestad and Wolff, 1991)

$$q_{\text{out}} = C_v z\sqrt{P^2 - P_{\text{out}}^2} \qquad [\text{mol/s}] \tag{4.3}$$

where $C_v[\,\frac{\text{mol}}{\text{Pa}\cdot\text{s}}]$ is the valve constant (dependent on type of gas), and z is the valve opening, $z \in [0, 1]$. It is assumed that the valve nominally has a time delay θ of 5 s, and not more than 7 s. Inserting the valve equation (4.3) into (4.2) gives the nonlinear model for the pressure in the tank

$$f(P, z) = \frac{dP}{dt} = \frac{RT}{V}q_{\text{in}} - \frac{RT}{V}C_v z\sqrt{P^2 - P_{\text{out}}^2} \qquad [\text{Pa/s}] \tag{4.4}$$

In order to derive SIMC-parameters for this model, a linear model is required. Linearizing (4.4) around an operation point $(*)$ using the Taylor expansion and neglecting higher order terms

$$f(x,u) \approx f(x^*,u^*) + \left.\frac{\partial f}{\partial x}\right|_* (x-x^*) + \left.\frac{\partial f}{\partial u}\right|_* (u-u^*) \tag{4.5}$$

gives the model in deviation variables

$$\dot{\tilde{P}} = a\tilde{P} + b\tilde{z} \tag{4.6}$$

where

$$a = \left.\frac{\partial f}{\partial P}\right|_* = -\frac{RT}{V} C_v z^* \frac{P^*}{\sqrt{P^{*2} - P_{out}^2}} \tag{4.7}$$

$$b = \left.\frac{\partial f}{\partial z}\right|_* = -\frac{RT}{V} C_v z^* \frac{P^*}{\sqrt{P^{*2} - P_{out}^2}} \tag{4.8}$$

Calculating the Laplace transform of (4.6), neglecting initial conditions and including the valve time delay, the first order transfer function is derived

$$g(s) = \frac{\tilde{P}(s)}{\tilde{z}(s)} = \frac{-\frac{b}{a}}{-\frac{1}{a}s + 1} = \frac{k}{\tau s + 1} e^{-\theta s} \tag{4.9}$$

To find the more robust tuning parameter τ_c, $k'_{\max}$ and $\theta_{\max}$ will need to be found. Noting that $k' = k/\tau = b$, $k'_{\max}$ is found as

$$k'_{\max} = -\frac{RT_{\max}}{V_{\min}} C_v z_{\max} \sqrt{{P_{\max}}^2 - P_{\text{out}}^2} \tag{4.10}$$

where $k'_{\max}$ is the largest absolute value of b. The nominal k' is

$$k'_{\text{nom}} = -\frac{RT_{\text{nom}}}{V_{\text{nom}}} C_v z_{\text{nom}} \sqrt{{P_{\text{nom}}}^2 - P_{\text{out}}^2} \tag{4.11}$$

The physical variables which change during operations are based on those in Skogestad and Wolff (1991) and are given in Table 4.1. The parameters which are assumed constant are listed in Table 4.2. Inserting the values in Table 4.1 and 4.2 into (4.11) gives

$$k'_{\text{nom}} = -2.2703 \cdot 10^5$$

The original SIMC parameters (2.2) with $\tau_c = \theta_{\text{nom}}$ are

$$\begin{aligned} K_c &= \frac{1}{k'_{\text{nom}}} \frac{1}{\tau_c + \theta_{\text{nom}}} = \frac{1}{k'_{\text{nom}}} \frac{1}{2\theta_{\text{nom}}} \\ \tau_I &= \min(\tau_{1,\,\text{nom}}, 8\theta_{\text{nom}}) \end{aligned} \tag{4.12}$$

Table 4.1: Operating conditions for the pressure tank.

Variable	Minium value	Nominal value	Maximum value
$V\,[\,\mathrm{m}^3]$	$20\,\mathrm{m}^3$	$75\,\mathrm{m}^3$	$100\,\mathrm{m}^3$
$P\,[\,\mathrm{Pa}]$	$62 \cdot 10^5\,\mathrm{Pa}$	$70 \cdot 10^5\,\mathrm{Pa}$	$90 \cdot 10^5\,\mathrm{Pa}$
$T\,[\,\mathrm{K}]$	$350\,\mathrm{K}$	$400\,\mathrm{K}$	$450\,\mathrm{K}$
$\theta\,[\,\mathrm{s}]$	$4\,\mathrm{s}$	$5\,\mathrm{s}$	$7\,\mathrm{s}$
z [fraction]	0.1	0.5	0.9

Table 4.2: Parameters in the pressure tank which are assumed constant.

Variable	Value
$C_v[\,\frac{\mathrm{mol}}{\mathrm{Pa\cdot s}}]$	$1.420 \cdot 10^{-3}\,\frac{\mathrm{mol}}{\mathrm{Pa\cdot s}}$
$r_{\mathrm{tank}}[\,\mathrm{m}]$	$3\,\mathrm{m}$

and inserting the value for k'_{nom} into (4.12) gives

$$\begin{aligned} K_c &= -4.40 \cdot 10^{-7} \\ \tau_I &= 16.3\,\mathrm{s} \end{aligned} \tag{4.13}$$

Note that the small gain is due to the pressure is given in [Pa] and not [bar]. The worst case scenario is when $V = 20\,\mathrm{m}^3$, $T = 450\,\mathrm{K}$, $P = 90 \cdot 10^5\,\mathrm{Pa}$ and $\theta = 7\,\mathrm{s}$. The more robust settings are calculated according to the procedure in Section 2.2 with $\tau_{c,\,\mathrm{worst\,case}} = 0$. Inserting the values in Tables 4.1 and 4.2 into (4.10) gives

$$k'_{\mathrm{max}} = -1.7820 \cdot 10^6$$

which gives the tuning parameter $\tau_c = 6.8\theta_{\mathrm{nom}}$. The robust controller parameters is thus

$$\begin{aligned} K_{c,\,\mathrm{robust}} &= \frac{1}{k'_{\mathrm{nom}}} \frac{1}{\tau_c + \theta_{\mathrm{nom}}} = \frac{1}{k'_{\mathrm{nom}}} \frac{1}{6.8\theta_{\mathrm{nom}}} = -1.12 \cdot 10^{-7} \\ \tau_I &= \min(\tau_{\mathrm{nom}}, 4(\tau_c + \theta_{\mathrm{nom}})) = \tau_{\mathrm{nom}} = 16.3\,\mathrm{s} \end{aligned} \tag{4.14}$$

Figure 4.2 shows the disturbance rejection (in-stream q_{in} is increased at $t = 500\,\mathrm{s}$) when operating with different process parameters. As expected, in the nominal case the original SIMC settings are better than the more conservative robust settings. For the worst case, the robust settings manages to control the system satisfactory, but the original SIMC settings becomes oscillatory with sustained oscillations. Figure 4.3 shows the response to a step in reference at $t = 500\,\mathrm{s}$. Since the pressure now changes, the SIMC settings becomes a little too aggressive also for the nominal case. For the worst case, the response becomes oscillatory as with the disturbance. The robust settings manage to control the process satisfactory for both nominal and worst cases.

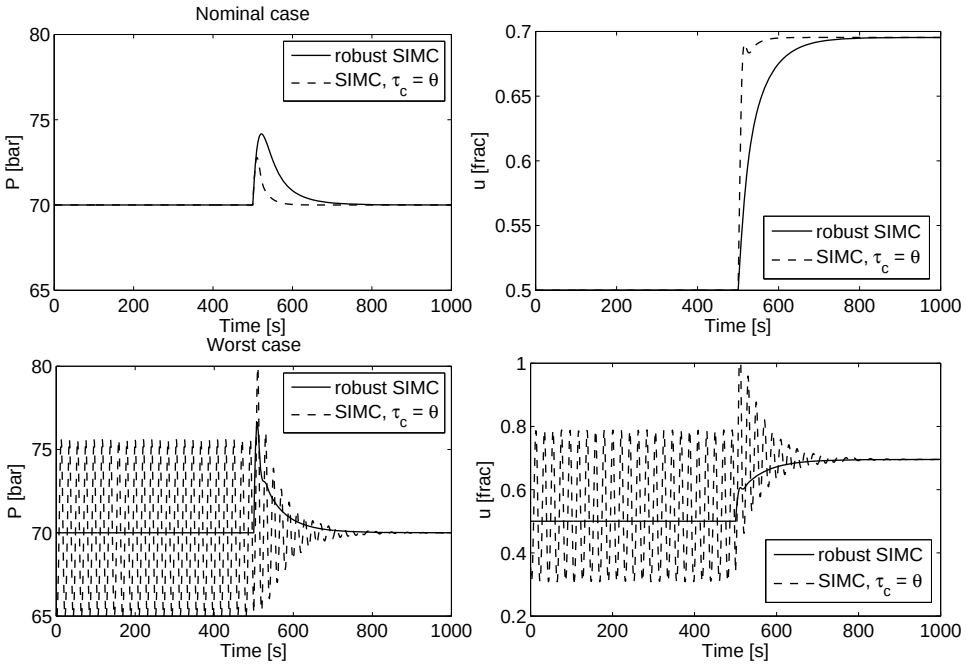

Figure 4.2: Comparison of disturbance rejection for the pressure tank.

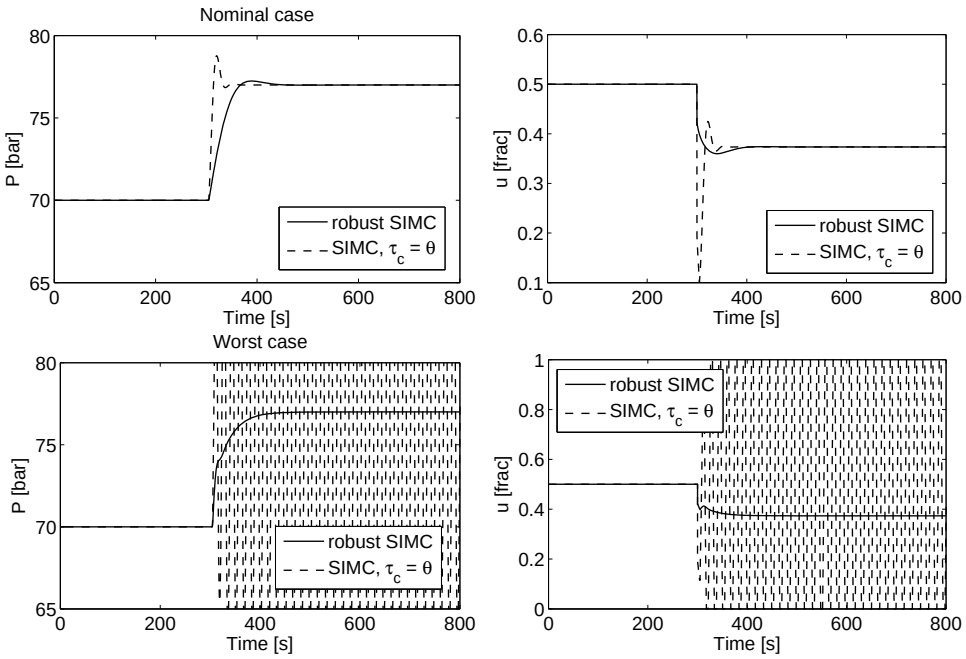

Figure 4.3: Comparison of response for step in reference for the pressure tank.

4.2 Modelling and control of level in an open tank

In this section, control of the liquid level in a open tank will be studied, as shown in Figure 4.4. The liquid stream in (q_{in}) is not controllable, and

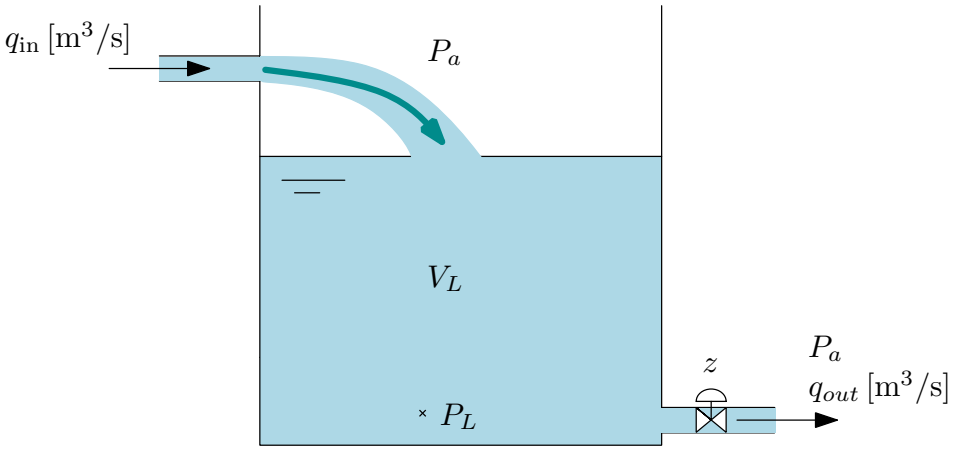

Figure 4.4: Level of liquid in an open tank.

viewed as a disturbance. The pressure at the downstream side of the valve in the out-stream (q_{out}) is atmospheric pressure: $P = P_a \approx 1\,\text{bar}$. The flow q_{out} is controlled by a valve with opening fraction z between 0 and 1.

The change in volume is the change of material, i.e. difference between inflow and outflow

$$\dot{V}_L = q_{\text{in}} - q_{\text{out}} \qquad [\text{m}^3/\text{s}] \tag{4.15}$$

The outflow of the valve can be represented by the equation (Skogestad and Wolff, 1991)

$$q_{\text{out}} = C_v z \sqrt{P_L - P_{\text{out}}} \qquad [\text{m}^3/\text{s}] \tag{4.16}$$

where $C_v[\,\text{m}^{3.5} \cdot \text{kg}^{-1/2}]$ is the valve constant (dependent on density ρ), and z is the valve opening, $z \in [0, 1]$. The time delay θ in the valve is also here assumed nominally to be 5 s. Assuming that the flow in the tank is neglectable, Bernoulli's equation (White, 2008) from the water surface to the bottom of the tank can be used to calculate the pressure at the bottom

$$\frac{p_1}{\rho} + \frac{1}{2}v_1^2 + gh_1 = \frac{p_2}{\rho} + \frac{1}{2}v_2^2 + gh_2 = \text{const} \tag{4.17}$$

With $P_{out} = P_a$ and $v_i \approx 0\,\text{m/s}$, (4.17) is simplified to

$$P_L = P_a + \rho g h = \rho g \frac{V_L}{A} \qquad [\text{Pa}] \tag{4.18}$$

Inserting (4.18) and (4.16) into (4.15), the nonlinear model for the level in the tank is derived

$$f(V_L, z) = \frac{dV_L}{dt} = q_{\text{in}} - k_1 z \sqrt{V_L} \qquad [\text{m}^3/\text{s}] \tag{4.19}$$

where $k_1 = C_v\sqrt{\frac{\rho g}{A}}$ The linearized model around $(V_L^*,\, z^*)$ is

$$\dot{\tilde{V}}_L = a\tilde{V}_L + b\tilde{z} \tag{4.20}$$

where

$$a = \left.\frac{\partial f}{\partial V_L}\right|_* = -\frac{1}{2}k_1\frac{z^*}{\sqrt{V_L^*}} \tag{4.21}$$

$$b = \left.\frac{\partial f}{\partial z}\right|_* = -k_1\sqrt{V_L^*} \tag{4.22}$$

Calculating the Laplace transform of (4.20), neglecting initial conditions and including time delay in the valve, gives the the first order transfer function

$$g_1(s) = \frac{-2V_L^*/z^*}{2\frac{\sqrt{V_L^*}}{kz^*}s + 1}e^{-\theta s} \tag{4.23}$$

and noting (as in Section 4.1) that $k' = b$, the nominal and maximum k' is found to be

$$\begin{aligned} k'_{\max} &= -k_1\sqrt{V_{L,\max}^*} \\ k'_{\text{nom}} &= -k_1\sqrt{V_{L,\text{nom}}^*} \end{aligned} \tag{4.24}$$

Table 4.3: Operating conditions for the open tank.

Variable	Minium value	Nominal value	Maximum value
$V_L\,[\,\mathrm{m}^3]$	$10\,\mathrm{m}^3$	$30\,\mathrm{m}^3$	$90\,\mathrm{m}^3$
$\theta\,[\,\mathrm{s}]$	$4\,\mathrm{s}$	$5\,\mathrm{s}$	$7\,\mathrm{s}$
$T[\,\mathrm{K}]$	–	$300\,\mathrm{K}$	–

Table 4.4: Physical parameters in the open tank which are assumed constant.

Variable	Value
$C_v[\,\mathrm{m}^{3.5}\cdot\mathrm{kg}^{-1/2}]$	$7.972\cdot10^{-3}\,\mathrm{m}^{3.5}\cdot\mathrm{kg}^{-1/2}$
$\rho\,[\,\mathrm{kg}/\,\mathrm{m}^3]$	$900\,\mathrm{kg}/\,\mathrm{m}^3$
$r_{\text{tank}}[\,\mathrm{m}]$	$3\,\mathrm{m}$

Using the same procedure as in the last section with the parameters and variable values from Tables 4.3 and 4.4 the values for k' are calculated to be

$$\begin{aligned} k'_{\text{nom}} &= -0.772 \\ k'_{\max} &= -1.336 \end{aligned}$$

which gives the SIMC parameters with $\tau_c = \theta$

$$K_c = -0.130$$
$$\tau_I = 40\,\mathrm{s}$$

and the the robust tuning parameter with $\tau_{c,\,\text{worst case}} = 0$ is found to be $\tau_c = 1.4\theta_{\text{nom}}$ giving

$$\begin{aligned} K_{c,\,\text{robust}} &= -0.107 \\ \tau_I &= 40\,\mathrm{s} \end{aligned} \tag{4.25}$$

Here the controller gains differ marginally, as opposed to the pressure tank. Response to a step change in liquid volume reference of $2\,\mathrm{m}^3$ at $t = 100\,\mathrm{s}$ for the nominal case and $35\,\mathrm{m}^3$ for the worst case is shown in Figure 4.5. The in-flow is $q_{\text{in}} = 0.5\,\mathrm{m}^3/\mathrm{s}$ with a step disturbance $d = 0.1\,\mathrm{m}^3/\mathrm{s}$ at $t = 300\,\mathrm{s}$. The main problem in the worst case is input saturation causing wind-up, rather than change in V_L. Therefore, the method of retuning will not give any advantage in this case. This is also expected, by comparing the different values for K_c which differs marginally, and the values for τ_I are identical.

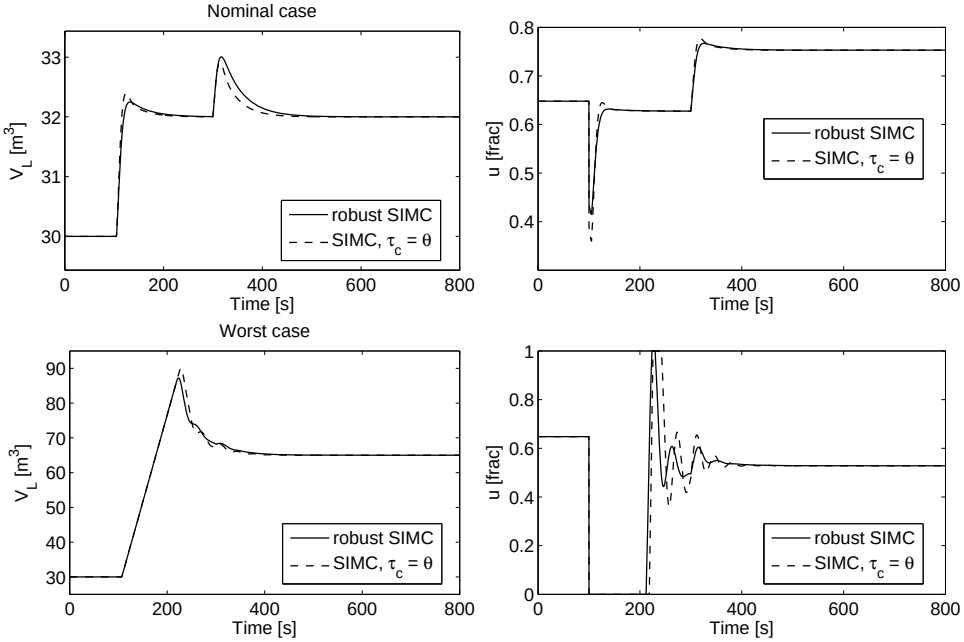

Figure 4.5: Comparison of response for step in reference and a step disturbance for the open tank.

4.3 Modelling and control of level in a closed tank

In Section 4.2 the control of liquid level in an open tank was studied. In this section the case where the tank is closed with $P \gg P_a$ will be studied where P_a is atmospheric pressure. An illustration of the tank is shown in Figure 4.6.

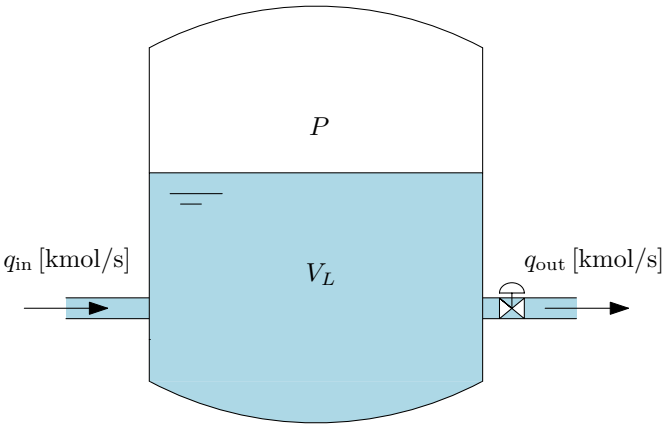

Figure 4.6: Level of liquid in a closed tank.

Now the pressure difference due to the liquid holdup can be neglected: $P_L = P + \rho g \frac{V_L}{A} \approx P$. Inserting this approximation in (4.16) gives

$$q_{\text{out}} = C_v z \sqrt{P - P_{\text{out}}} \qquad [\text{m}^3/\text{s}] \tag{4.26}$$

It is assumed that the pressure inside the tank is larger than the outlet pressure, and that this pressure is much larger than atmospheric pressure: $P_L > P_{out} \gg P_a$. Doing the same calculations as in Section 4.2, neglecting initial conditions and including the valve time delay, the transfer function in deviation variables from $\tilde{z}$ to $\tilde{V}_L$ is found to be

$$g_2(s) = \frac{\tilde{V}_L(s)}{\tilde{z}(s)} = \frac{-C_v\sqrt{P^* - P_{\text{out}}}}{s} e^{-\theta s} = \frac{k'}{s} e^{-\theta s} \tag{4.27}$$

where $k' = -C_v\sqrt{P^* - P_{\text{out}}}$. We thus have

$$\begin{aligned} k'_{\text{max}} &= -C_v\sqrt{P^*_{\text{max}} - P_{\text{out}}} \\ k'_{\text{nom}} &= -C_v\sqrt{P^*_{\text{nom}} - P_{\text{out}}} \end{aligned} \tag{4.28}$$

Comparing $g_1(s)$ in (4.23) and $g_2(s)$ in (4.27) we can see that the process has changed from a first order model to a pure integrating model. This is because the self-regulating effect the liquid level has is so small that it is neglected in the model.

The gas inventory is assumed constant, as well as the temperature in the tank. Thus, using the ideal gas law (4.1) with n and T constant gives

$$P_{\max} = \frac{P_{\text{nom}}(V_{\text{tank}} - V_{L,\,\text{nom}})}{V_{\text{tank}} - V_{L,\,\max}} \tag{4.29}$$

From (4.29) the maximum expected pressure can be calculated, which will be used to find k'_{max}. The operating conditions are given in Table 4.5. From

Table 4.5: Operating conditions for the closed tank.

Variable	Minium value	Nominal value	Maximum value
$V_L\,[\,\text{m}^3]$	$10\,\text{m}^3$	$50\,\text{m}^3$	$65\,\text{m}^3$
$\theta\,[\,\text{s}]$	$4\,\text{s}$	$5\,\text{s}$	$7\,\text{s}$
$T[\,\text{K}]$	–	$400\,\text{K}$	–

these conditions, and a tank size $V_{\text{tank}} = 100\,\text{m}^3$, the maximum expected pressure can be calculated

$$P_{\max} = \frac{70 \cdot 10^5\,\text{Pa} \cdot (100\,\text{m}^3 - 50\,\text{m}^3)}{100\,\text{m}^3 - 65\,\text{m}^3} = 100 \cdot 10^5\,\text{Pa}$$

The parameters which are assumed constant are the same as with the open tank, given in Table 4.4. Inserting the value for C_v, the calculated maximum pressure and the nominal pressure in (4.28) gives

$$k'_{\text{nom}} = -7.97$$
$$k'_{\max} = -15.94$$

The time delay θ is assumed the same as with the open tank, but the liquid holdup V_L is changed to $50\,\text{m}^3$ for the nominal case, and $65\,\text{m}^3$ for the worst case. The original SIMC settings with $\tau_c = \theta_{\text{nom}}$ is

$$K_c = -0.0125$$
$$\tau_I = 40\,\text{s}$$

Using the procedure from Section 2.2 with $\tau_{c,\,\text{wc}} = 0$, τ_c is found to be $\tau_c = 1.8\theta_{\text{nom}}$ which gives

$$K_c = -0.009$$
$$\tau_I = 56\,\text{s}$$

The tank is simulated with a step in reference for V_L of $50\,\text{m}^3 - 52\,\text{m}^3$ for the nominal case and $50\,\text{m}^3 - 60\,\text{m}^3$ for the worst case. The disturbance is the same as with the open tank, and the response is shown in Figure 4.7. As opposed to the open tank, in this case the detuning has a noticeable effect

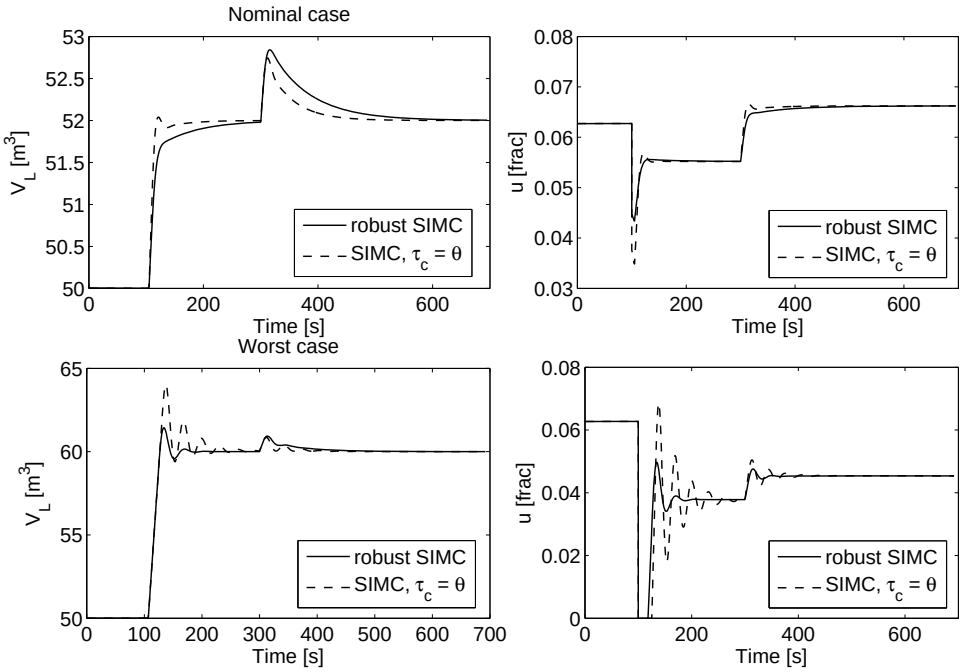

Figure 4.7: Compare response for step in reference and a step disturbance for the closed tank.

for the worst case. Some signs of oscillations are present (due to $\tau_{c,\,\mathrm{wc}} = 0$), but the response is much better than the case with $\tau_c = \theta_{\mathrm{nom}}$. At the same time, the performance for the nominal case is not noticeably reduced. The reason for both of these properties being fulfilled is that the variation in conditions for worst case and nominal case is not too large (k' is doubled for the worst case, and θ changes from 5 s to 7 s).

This is an integrating process, which can be seen from (4.27). In Section 2.2 it was mentioned that $\tau_{c,\,\mathrm{wc}} = 0$ may be a bit too aggressive for integrating processes. In Figure 4.7 this can be seen from the small oscillations for the worst case. When choosing $\tau_{c,\,\mathrm{wc}}$ there is a performance trade-off in nominal and worst case operation. In this case, an increase in $\tau_{c,\,\mathrm{wc}}$ may lead to a too slow response for the nominal case, but this will at the same time reduce oscillations for the worst case.

4.4 Two-phase tank model

In this section, an analytic model for the two-phase tank in Skogestad and Wolff (1991) shown in Figure 4.8 will be derived. For ease of modelling, the inlet streams are modelled as two independent streams containing only gas and liquid respectively. Further, condensation or vaporization are neglected, and it is assumed that separation is complete and that the gas stream out does not contain any liquid and vice versa. This example has also been briefly discussed in Skogestad and Postlethwaite (2005), but the discussion in this chapter will be much more thorough, with emphasis on robust control.

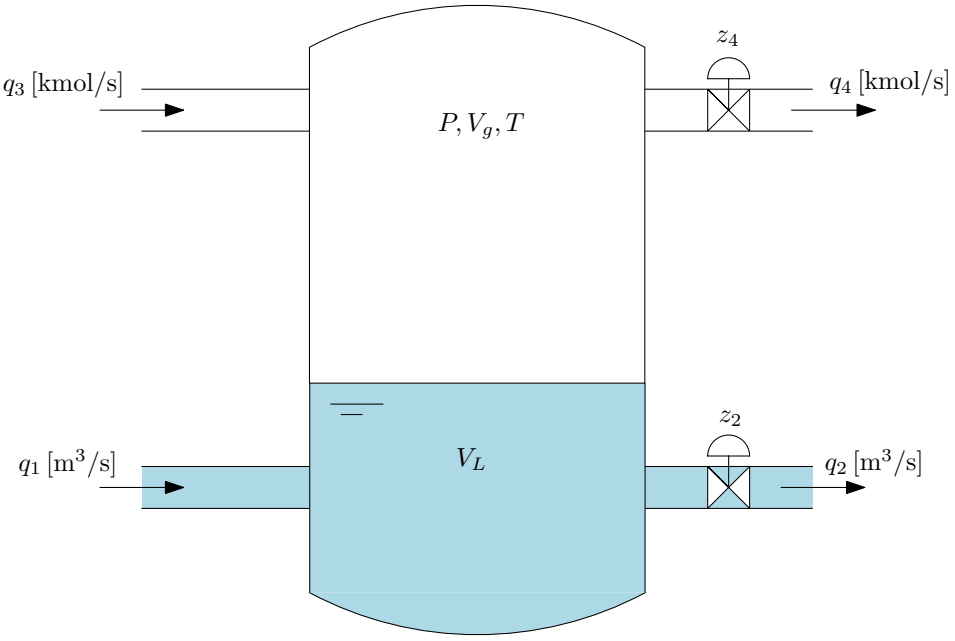

Figure 4.8: The two-phase high pressure vessel.

Table 4.6: Nominal steady-state operating conditions for the two-phase tank.

Variable	Value	Variable	Value
V_L	$20\,\mathrm{m}^3$	z_1	0.5
P	$70 \cdot 10^5\,\mathrm{Pa}$	z_2	0.5
P_L	$70.07 \cdot 10^5\,\mathrm{Pa}$	q_1	$4\,\mathrm{m}^3/\mathrm{s}$
P_{GO}	$60 \cdot 10^5\,\mathrm{Pa}$	q_3	$2.56\,\mathrm{kmol/s}$
P_{LO}	$60 \cdot 10^5\,\mathrm{Pa}$	T	$400\,\mathrm{K}$

Table 4.7: Process parameters and constraints for the two-phase tank.

Variable	Value
C_{v2}	$7.973 \cdot 10^{-3}$
C_{v4}	$1.420 \cdot 10^{-3}$
V_{tank}	$100\,\text{m}^3$
$P_{\max}$	$100 \cdot 10^5\,\text{Pa}$
z_i	$[0, 1]$

4.4.1 Material balances

The material balances will be the same as in Sections 4.1 and 4.3 but with added indices. Thus, they are repeated in the following with correct indices corresponding to Figure 4.8.

The change in volume for an incompressible fluid is the difference between flow in and out

$$\frac{dV_L}{dt} = q_1 - q_2 \qquad [\,\text{m}^3/\,\text{s}] \tag{4.30}$$

As in Section 4.3, differentiating the ideal gas law with respect to time gives

$$\dot{P}V_g + P\dot{V_g} = \dot{n_g}RT_g + n_gR\dot{T_g} \tag{4.31}$$

Neglecting temperature dynamics gives $\dot{T} = 0$. Rearranging, and using that $V_g = V_{\text{tank}} - V_L\,[\,\text{m}^3]$ and $\dot{n_g} = q_3 - q_4\,[\,\text{mol}/\,\text{s}]$, gives

$$\frac{dP}{dt} = \frac{RT}{V_{\text{tank}} - V_L}(q_3 - q_4) + \frac{P}{V_{\text{tank}} - V_L}(q_1 - q_2) \qquad [\,\text{Pa}/\,\text{s}] \tag{4.32}$$

4.4.2 Valve equations

The valve equations are the same as used in Sections 4.1 and 4.3 but with added indices. They are given by

$$q_2 = C_{v2} \cdot z_2\sqrt{P_L - P_{LO}} \qquad [\,\text{m}^3/\,\text{s}] \tag{4.33}$$

$$q_4 = C_{v4} \cdot z_4\sqrt{P^2 - P_{GO}^2} \qquad [\,\text{mol}/\,\text{s}] \tag{4.34}$$

where P is the pressure of the gas, $P_L = P + \rho g V_L/A$ is the pressure in the bottom of the tank, P_{LO} is the downstream liquid pressure and P_{GO} is downstream gas pressure. Cv_i are valve constants, and z_i are the valve openings, $z_i \in [0, 1]$.

4.4.3 Linear model of the tank

Given the nonlinear model

$$\begin{aligned} \dot{x} &= f(x,u,d) \\ y &= h(x,u,d) \end{aligned} \tag{4.35}$$

the linearized model, given stationary point (x^*, u^*, d^*), is given in deviation variables

$$\dot{\tilde{x}} = A\tilde{x} + B\tilde{u} + B_d\tilde{d} \tag{4.36}$$

where

$$A = \frac{\partial f}{\partial x}(x,u,d)\bigg|_*; \quad B = \frac{\partial f}{\partial u}(x,u,d)\bigg|_*; \quad B_d = \frac{\partial f}{\partial d}(x,u,d)\bigg|_* \tag{4.37}$$

The linearized model of the tank using (4.30) and (4.32) with

$$x = \begin{bmatrix} V_L \\ P \end{bmatrix}, \quad u = \begin{bmatrix} z_2 \\ z_4 \end{bmatrix}, \quad d = \begin{bmatrix} q_1 \\ q_3 \end{bmatrix} \tag{4.38}$$

is given by

$$\begin{aligned}
A_{11} = \frac{\partial f_1}{\partial x_1} &= \frac{-C_{v2}\rho g u_1^*}{2A\sqrt{x_2^* - P_{LO} + \frac{\rho g}{A}x_1^*}} \\
A_{12} = \frac{\partial f_1}{\partial x_2} &= \frac{-C_{v2}u_1^*}{2\sqrt{x_2^* - P_{LO} + \frac{\rho g}{A}x_1^*}} \\
A_{21} = \frac{\partial f_2}{\partial x_1} &= \frac{RT}{(V - x_1^*)^2}\left(d_2^* - C_{v4}u_2^*\sqrt{x_2^{*2} - P_{GO}^2}\right) \\
&\quad + \frac{x_2^*}{(V - x_1^*)^2}\left(d_1^* - C_{v2}u_1^*\sqrt{x_2^* - P_{LO} + \frac{\rho g}{A}x_1^*}\right) \\
&\quad - \frac{x_2^*}{V - x_1^*}\frac{\rho g C_{v2}u_1^*}{2A\sqrt{x_2^* - P_{LO} + \frac{\rho g}{A}x_1^*}} \\
A_{22} = \frac{\partial f_2}{\partial x_1} &= -\frac{RTx_2^*}{V - x_1^*}\frac{C_{v4}u_2^*}{\sqrt{x_2^{*2} - P_{GO}^2}} \\
&\quad + \frac{1}{V - x_1^*}\left(d_1^* - C_{v2}u_1^*\sqrt{x_2^* - P_{LO} + \frac{\rho g}{A}x_1^*}\right) \\
&\quad - \frac{x_2^*}{V - x_1^*}\frac{C_{v2}u_1^*}{2\sqrt{x_2^* - P_{LO} + \frac{\rho g}{A}x_1^*}}
\end{aligned}$$

$$
\begin{aligned}
B_{11} &= \frac{\partial f_1}{\partial x_1} = -C_{v2}\sqrt{x_2^* - P_{LO} + \frac{\rho g}{A}x_1^*} \\
B_{12} &= \frac{\partial f_1}{\partial x_2} = 0 \\
B_{21} &= \frac{\partial f_2}{\partial x_1} = -\frac{x_2^*}{V - x_1^*}C_{v2}\sqrt{x_2^* - P_{LO}} \\
B_{22} &= \frac{\partial f_2}{\partial x_2} = -\frac{RT}{V - x_1^*}C_{v4}\sqrt{x_2^{*2} - P_{GO}^2}
\end{aligned}
$$

$$
\begin{aligned}
B_{d,11} &= \frac{\partial f_1}{\partial x_1} = 1 \\
B_{d,12} &= \frac{\partial f_1}{\partial x_2} = 0 \\
B_{d,21} &= \frac{\partial f_2}{\partial x_1} = \frac{x_2^*}{V - x_1^*} \\
B_{d,22} &= \frac{\partial f_2}{\partial x_2} = \frac{RT}{V - x_1^*}
\end{aligned}
$$

where it is assumed that P_{GO} and P_{LO} are constant. Assuming that both state variables are measurable gives

$$C = \begin{bmatrix} 1 & 0 \\ 0 & 1 \end{bmatrix} \tag{4.39}$$

Calculating the Laplace transform and neglecting initial conditions as in Sections 4.1−4.3, the system can be written on the form

$$y = G(s)u + G_d(s)d \tag{4.40}$$

where

$$G(s) = C(sI - A)^{-1}B; \qquad G_d(s) = C(sI - A)^{-1}B_d \tag{4.41}$$

Inserting the steady-state values from Table 4.6 and process constants from Table 4.7 in addition to include the time delays of the valves gives

$$G(s) = \frac{e^{-5s}}{(s + 1.73 \cdot 10^{-4})(s + 0.232)} \begin{bmatrix} -8.0s - 0.4584 & 0.4227 \\ -7.0 \cdot 10^5 s - 1.942 & -2.128 \cdot 10^5 s - 146.7 \end{bmatrix} \tag{4.42}$$

$$G_d(s) = \frac{e^{-5s}}{(s + 1.73 \cdot 10^{-4})(s + 0.232)} \begin{bmatrix} s + 0.0573 & -8.257 \cdot 10^{-5} \\ 8.75 \cdot 10^4 s + 0.2428 & 41.57s + 0.02865 \end{bmatrix} \tag{4.43}$$

where minimal realization (`minreal`) in MATLAB is used. The rank of the controllability and observability matrices are 2, meaning that the linearized models are both controllable and observable (Chen, 1999).

To calculate the SIMC settings for a PI controller, the elements in the linearized model (4.42) need to be reduced to a first order plus time delay process, or a pure integrating plus time delay process. The half-rule described in Section 2.1 is a systematic way to find the model reductions, but the frequency domain where the reduction is most correct may not lie inside the bandwidth ω_B where the models needs to be most correct, because $\omega < \omega_B$ is loosely speaking the frequency where control is effective (Skogestad and Postlethwaite, 2005). Thus, the reduction is altered some, in order to get a good model for these frequencies. Dependent of the choice of controllers $k_i(s)$, ω_B will lie around 10^{-3} (this will be discussed later). With this requirement the reduced model is found to be

$$G(s) \approx \begin{bmatrix} \frac{-1.72}{s}e^{-5s} & \frac{1.79}{s}e^{-7.10s} \\ \frac{-3.01\cdot 10^6}{4.31s+1}e^{-5s} & \frac{-3.67\cdot 10^6}{17.24s+1}e^{-5s} \end{bmatrix} \tag{4.44}$$

For the worst case conditions given in Table 4.8, the linearized model around the new operating point with $z_i^* = 0.35$ is given by

$$G_{\text{wc}}(s) = \frac{e^{-5s}}{(s+5.28\cdot 10^{-6})(s+0.313)} \begin{bmatrix} -11.34s - 1.00 & 0.8755 \\ -2.59\cdot 10^6 s + 328.4 & -8.93\cdot 10^5 s - 303.8 \end{bmatrix} \tag{4.45}$$

which is reduced, in the same way as above, to

$$G_{\text{wc}}(s) \approx \begin{bmatrix} \frac{-3.16}{s}e^{-7s} & \frac{2.80}{s}e^{-8.60s} \\ \frac{9.37\cdot 10^6}{3.195s+1}e^{-8.60s} & \frac{-2.858\cdot 10^6}{3.195s+1}e^{-7s} \end{bmatrix} \tag{4.46}$$

4.4.4 Decentralized control of the tank

The setpoint changes and disturbances for the nominal and worst case, are listed in Table 4.8. As mentioned, to use the SIMC tuning rules, the reduced

Table 4.8: Setpoint changes and disturbances.

Variable	Nominal case	Worst case	Time of occurrence
$V_L\,[\,\mathrm{m}^3]$	$20 - 21\,\mathrm{m}^3$	$60 - 65\,\mathrm{m}^3$	100 s
$P\,[\,\mathrm{Pa}]$	$70\cdot 10^5\,\mathrm{Pa}$	$70\cdot 10^5 - 80\cdot 10^5\,\mathrm{Pa}$	600 s
$d_1\,[\,\mathrm{m}^3/\,\mathrm{s}]$	$0.4\,\mathrm{m}^3/\,\mathrm{s}$	$0.4\,\mathrm{m}^3/\,\mathrm{s}$	300 s
$d_2\,[\,\mathrm{mol}/\,\mathrm{s}]$	$0.5\,\mathrm{kmol}/\,\mathrm{s}$	$0.5\,\mathrm{kmol}/\,\mathrm{s}$	900 s
$T\,[\,\mathrm{K}]$	400 K	450 K	-

model in (4.44) must be used. If $\tau_{ci} = \theta$ is used for the diagonal pairing, loop 1 will get a crossover frequency of $\omega_c = 0.4$. With a phase margin of 30° and a delay $\theta = 5\,\text{s}$, the maximum ω_c is bounded by $\omega_c \leq \frac{0.5}{\theta} \approx 0.1$, see Appendix A.2. This is obtained by using $\tau_{c1} = 3\theta$. For loop 2, this bound is obtained with $\tau_{c2} = \theta$. Plotting the singular values, ω_B, which is the frequency where $\bar{\sigma}(S(j\omega))$ crosses $\frac{1}{\sqrt{2}}$ from below (see Appendix A.2), is found from Figure 4.9 to be $\omega_B = 0.0002$.

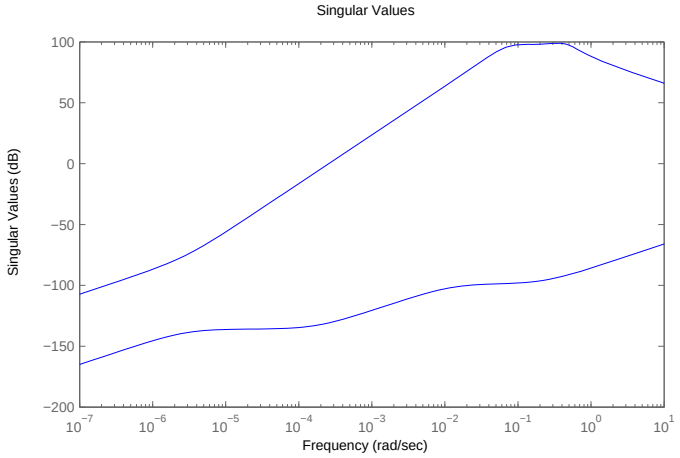

Figure 4.9: Singular values for $S(j\omega)$ when $\tau_{c1} = 3\theta$ and $\tau_{c2} = \theta$.

When choosing paring, Skogestad and Postlethwaite (2005) recommends to pair such that the RGA is close to identity at the frequencies around the closed-loop bandwidth. The magnitude of the RGA elements for the nominal case is shown in Figure 4.10 (the gains will be similar for the worst case, but with a larger magnitude of $|\lambda_{11}| = |\lambda_{22}|$ for small frequencies).
For the nominal case with $\omega_B = 0.0002$ the RGA is

$$\Lambda_{\text{nom}}(j\omega_B) = \begin{bmatrix} 0.564 - 0.365i & 0.436 + 0.365i \\ 0.436 + 0.365i & 0.564 - 0.365i \end{bmatrix}$$

so pairing on the diagonal elements is probably slightly better since these elements are closest to 1. The RGA for the worst case at $\omega_B = 0.0002$ is (the bandwidth is not changed any significantly from nominal to worst case)

$$\Lambda_{\text{wc}}(j\omega_B) = \begin{bmatrix} 0.374 - 0.310i & 0.626 + 0.310i \\ 0.626 + 0.310i & 0.374 - 0.310i \end{bmatrix}$$

so apparently, pairing on the off-diagonal might be a better choice overall. In practice, this means that the pressure is controlled by level measurements and vice versa. The pairing will still be done on the diagonal elements, since this will make it possible to compare this example with the SISO examples in the last sections.

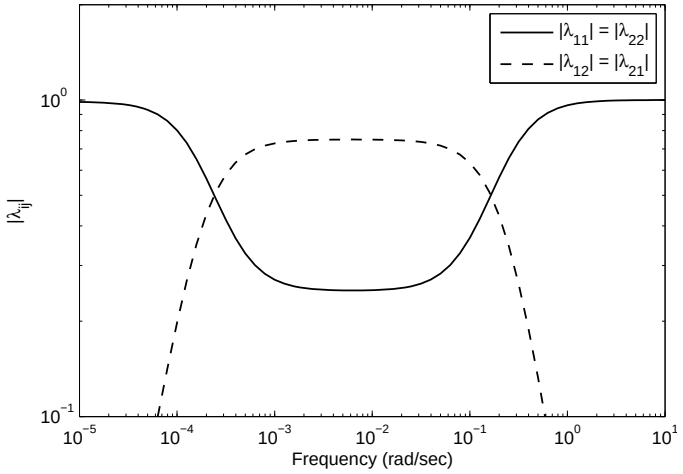

Figure 4.10: Magnitude of RGA elements in the nominal case.

With the tuning settings found above

$$\begin{aligned} \tau_{c1} &= 3\theta \\ \tau_{c2} &= \theta \end{aligned}$$

the SIMC PI controller parameters, using the diagonal elements of (4.42), is found to be

$$\begin{aligned} K_{c1} &= -0.0285 \\ \tau_{i1} &= 80\,\mathrm{s} \\ K_{c2} &= -4.70 \cdot 10^{-7} \\ \tau_{i2} &= 17.2\,\mathrm{s} \end{aligned} \tag{4.47}$$

and the simulations for the nominal and worst case is shown in Figures 4.11 and 4.12, labeled SIMC. The selected tuning is based on the nominal case without consideration for the worst case. Hence, the response is good for the nominal case, but for the worst case the response becomes unsatisfactory oscillatory. Especially after the step in pressure reference at $t = 600\,\mathrm{s}$ where there are sustained oscillations in both level and pressure.

To find the robust settings, the procedure from Section 2.2 is used on the diagonal elements of the nominal reduced model (4.44) and the worst case reduced model (4.46). The worst case-tuning parameters are chosen to be

$$\begin{aligned} \tau_{c1,\,\mathrm{wc}} &= 2\theta_{\mathrm{nom}} \\ \tau_{c2,\,\mathrm{wc}} &= 0 \end{aligned}$$

based on the tuning parameters of $\tau_{c1} = 3\theta_{\mathrm{nom}}$ and $\tau_{c2} = \theta_{\mathrm{nom}}$ for the regular

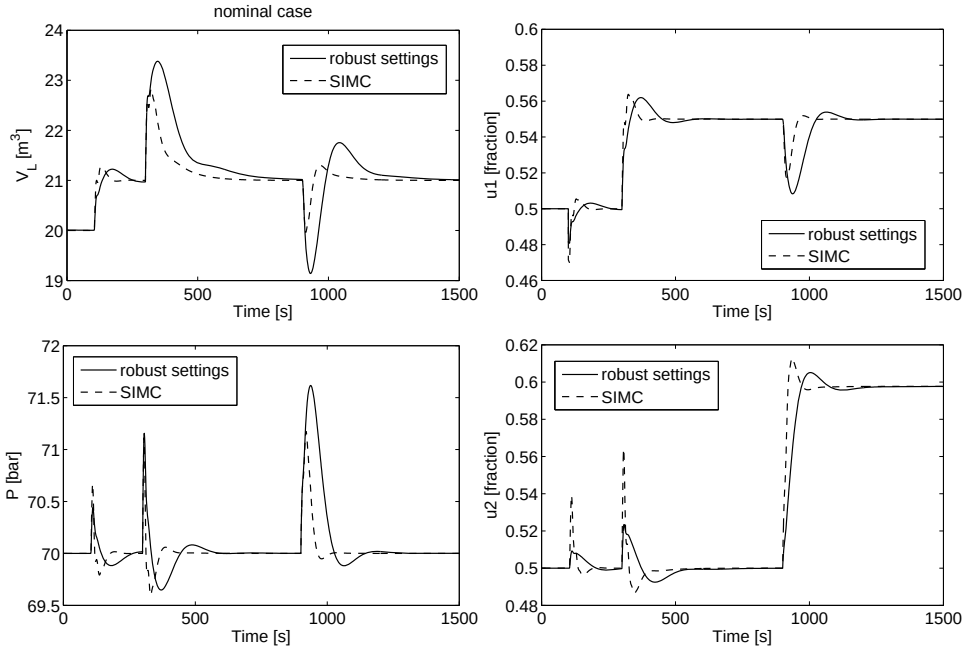

Figure 4.11: Comparison of regular SIMC settings and robust settings for nominal operation of the tank.

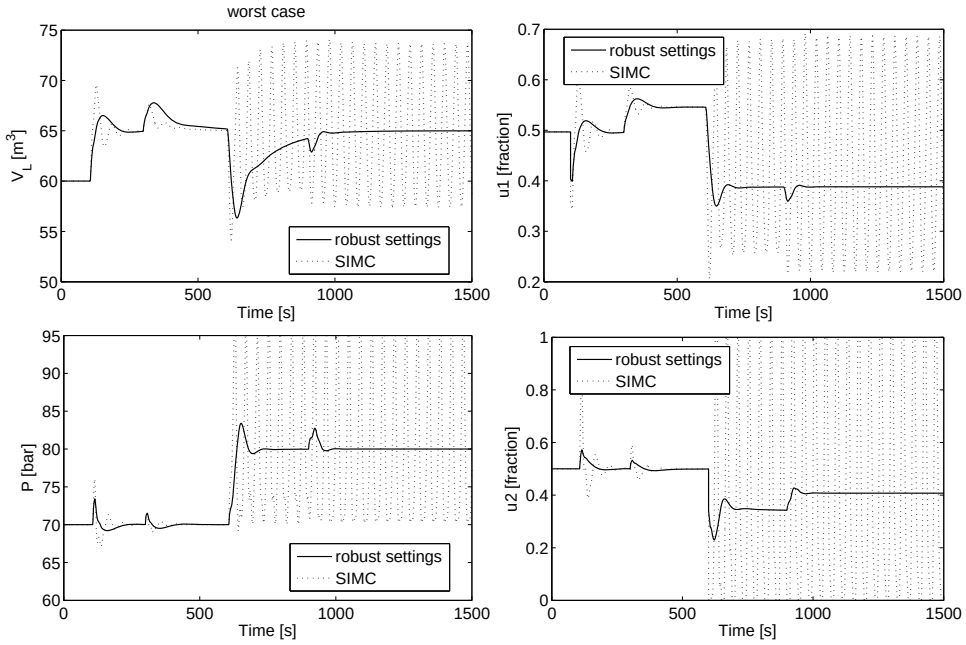

Figure 4.12: Comparison of regular SIMC settings and robust settings for worst case operation of the tank.

SIMC-tunings. These parameters gives the tuning parameters

$$\begin{aligned}\tau_{c1} &= 5.12\theta_{\text{nom}} \\ \tau_{c2} &= 4.88\theta_{\text{nom}}\end{aligned}$$

which gives the PI controller parameters

$$\begin{aligned}K_{c1} &= -0.0186 \\ \tau_{i1} &= 122.5\,\text{s} \\ K_{c2} &= -1.60 \cdot 10^{-7} \\ \tau_{i2} &= 17.2\,\text{s}\end{aligned} \tag{4.48}$$

The response of the parameters in (4.48) and (4.47) are shown in Figures 4.11 and 4.12. From these figures, the robust settings are little slower with poorer disturbance rejection than the regular tunings for the nominal case, but for the worst case the regular tuning settings makes the process oscillatory as mentioned earlier. When there is a step change in pressure reference (from 70 bar to 80 bar), both loops gets large sustained oscillations for the regular tunings, while the robust tunings has a good response for both loops (though the level control is a bit slow when counteracting influences from pressure). By including information about the worst case, this shows that it is possible to design controllers which handles both cases satisfactory. Even if the control is good in sense of robustness for changes in operating conditions, the interactions are still quite large. This can especially be seen by the effect a pressure step reference and a disturbance in the gas inflow has on the level. In the following section, this effect will be tried to be reduced using a one-way decoupler.

4.4.5 Reducing interactions with a one-way decoupler

To minimize the effect of interactions, decoupling was found to be a good method in Chapter 3. In particular, inverted decoupling and one-way decoupling seemed to be the best alternatives for the robustness requirements. Since the one-way decoupler is the simplest, but yet a good decoupling technique, it will be used on the tank. From Figures 4.11 and 4.12 pressure seems to affect level more than vice versa, thus a one-way decoupler will be used from u_2 (valve opening for the gas-stream out) to the controller c_1 in loop 1 (the level controller). In this section, only the robust tuning settings (4.48) will be used.

Using the one-way decoupler described in Section 2.4.4 from u_2 to c_1 (i.e. setting $D_{21} = 0$ in Figure 2.4), the decoupler element based on the model (4.42) from the nominal case is

$$D_{12}(s) = -\frac{G_{12}(s)}{G_{22}(s)} = \frac{0.922}{17.2s + 1} \tag{4.49}$$

To test the decoupler, the conditions used as nominal case conditions in the last sections are used, but a step pressure reference from 70 bar to 80 bar is added. This is to best illustrate the effect the decoupling has. The one-way decoupler is compared with decentralized control in Figure 4.13. At the step in pressure reference ($t = 600\,\mathrm{s}$) the decoupler manage to counteract much of the influence of the pressure change, whereas with decentralized control there is a large drop in the level. At $t = 900\,\mathrm{s}$ there is a load disturbance in the gas inflow. The effect of this disturbance is not reduced by the one-way decoupler because the disturbance enters the process outside the scope of the decoupler. If it is important to reduce the effect of this disturbance, one solution is to use feed-forward from the disturbance d_2 to the level controller output c_1.

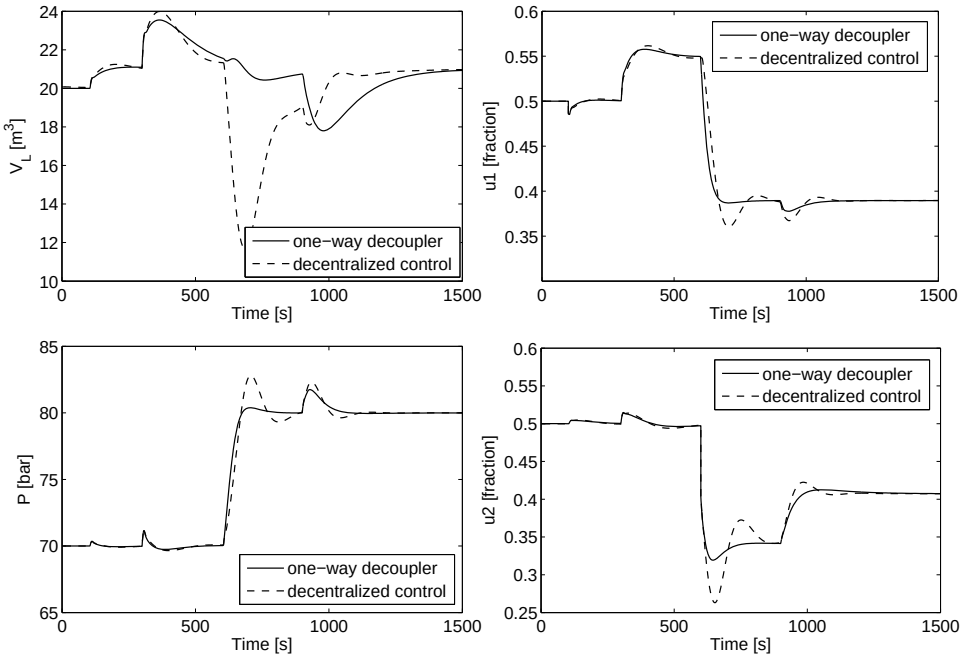

Figure 4.13: Compare one-way decoupler with decentralized control.

4.4.6 The effect of input saturation

In Section 4.3 it was found that the liquid level in a high-pressure tank behaves like an integrating process. Therefore, if the level control is taken out of service the tank will either fill up or be drained assumed that the inflow is kept constant. The pressure on the other hand, was found in Section 4.1 to be self-regulating. In this section the effect of input saturation in both the level control valve and the pressure control valve for decentralized control and the one-way decoupler will be studied. In the simulations in the previous sections, the valves were limited to $u_i \in [0, 1]$ which will be labeled

'no decoupler' in the figures in this section. This is because these limits were not met in the simulations in the previous chapters.

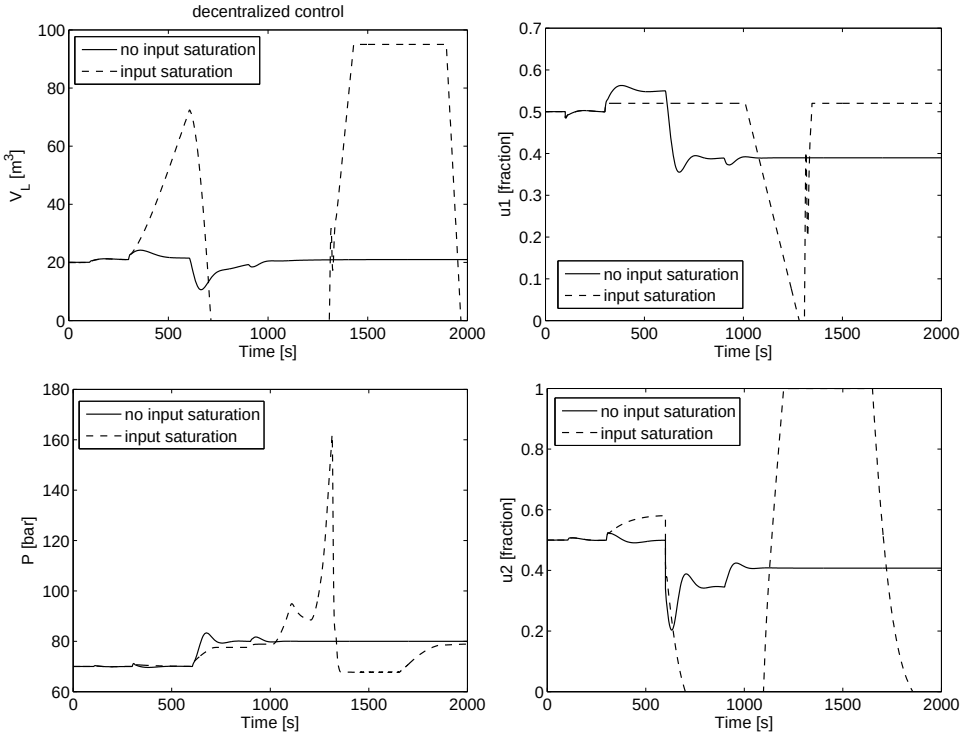

Figure 4.14: Input saturation in the level control valve u_1 with decentralized control.

Starting with the input saturation

$$u_1 \in [0, 0.52]$$

in the liquid control valve, the response for decentralized control is shown in Figure 4.14 and for one-way decoupler in Figure 4.15. In order to get loop 2 to be robust against input saturation in u_1, the effect of the saturation should be small. For the one-way decoupler this is almost satisfied (Figure 4.15). The control works good until u_2 goes into saturation around $t = 700\,\text{s}$, but control is never lost and for $t > 1500\,\text{s}$ pressure follows the reference. The decentralized controllers (Figure 4.14) more or less looses control of the pressure with a peak-value of around 160 bar, which is much larger than the specified max pressure of 100 bar. The main problem with saturation in level control valve is that, as mentioned above, the level is an integrating process, thus the tank is either filled or drained when there is loss of control. Note that the one-way decoupler managed to control the system even if there were no decoupling from the saturated u_1 to pressure control c_2.

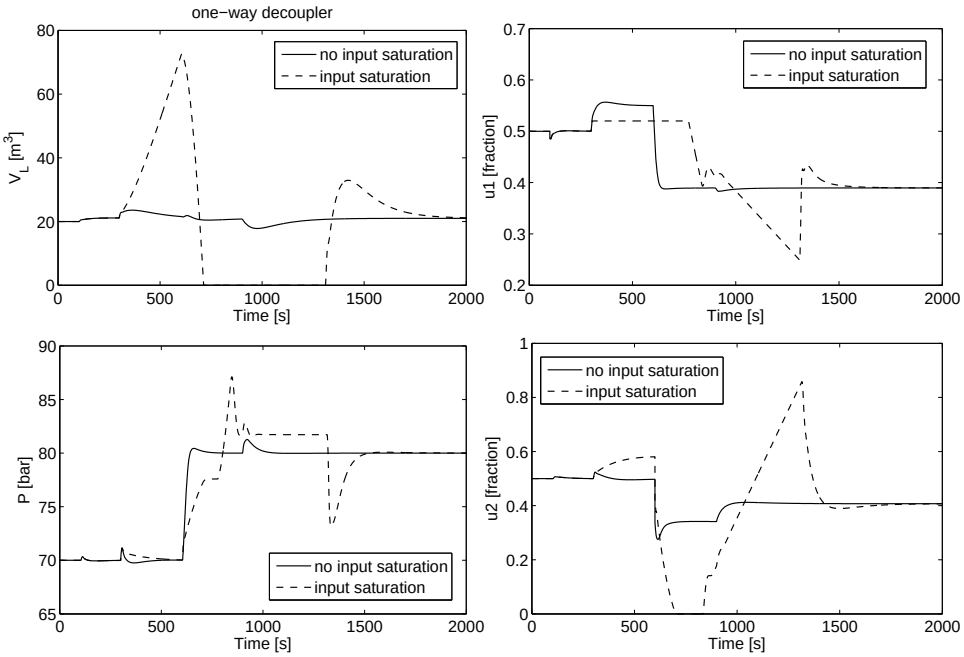

Figure 4.15: Input saturation in the level control valve u_1 with one-way decoupler.

Next, the effect of the input saturation

$$u_2 \in [0, 0.45]$$

in the pressure control valve will be studied. For decentralized control, the response is shown in Figure 4.16. Saturation in u_2 actually reduces the effect changes in pressure reference has on the level. This is because the pressure changes much slower due to the saturation, as can be seen in the pressure plot in Figure 4.16. Since the pressure is self-regulating, the process will not be destabilized by setting u_2 in open loop, as long as the valve is not closed (or nearly closed) and that this does not make u_1 go into saturation. The response with the one-way decoupler is shown in Figure 4.17. Here there is no noticeable effect of saturation in u_2 on the response for V_L. There is still a problem with the disturbance d_2 in gas inflow as described above.

In this section, it is shown that input saturation can be handled by decentralized control when independent design is used, for the cases when the processes are self-regulating, but not for integrating processes. The one-way decoupler manages to control the system satisfactory even if the saturated input is not the one which is decoupled. Also, the decoupling element (4.49) is quite simple.

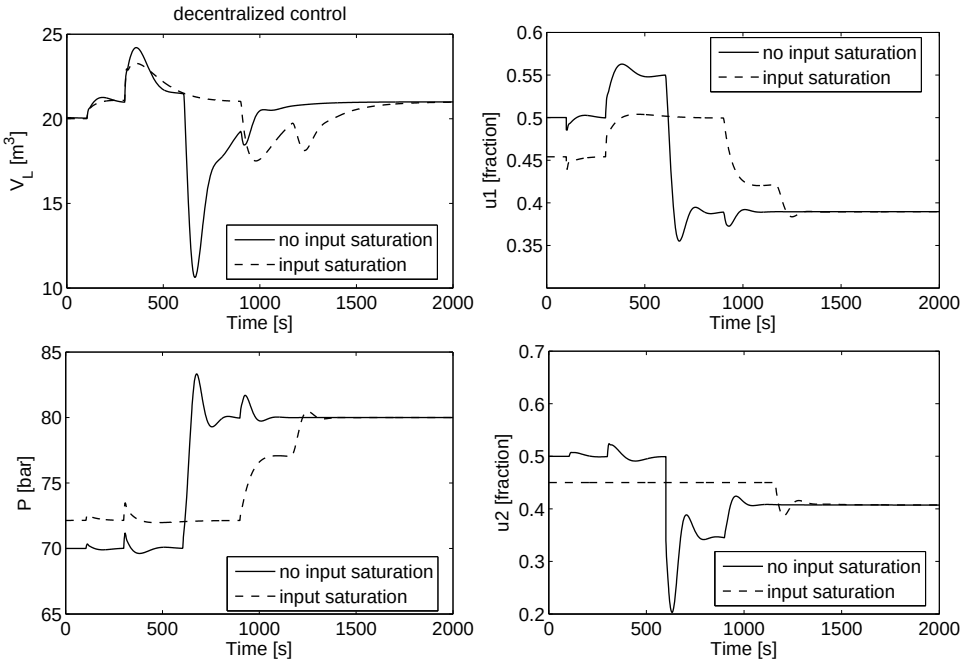

Figure 4.16: Input saturation in the pressure control valve u_2 with decentralized control.

4.5 Use of cascade control

Inspecting (4.30) and (4.33) it is evident that the interaction from pressure to level is due to the flow through the liquid out-stream q_2, which is both dependent on valve opening z_2 and pressure P in the tank. By using a flow controller in cascade with the level controller, the process becomes lower triangular since (4.30) no longer is depend on P. This is a similar case the the apparent process with one-way decoupler. This illustrates that a smart selection of controllers can ease control of the system. Since the scope of this report is to look into how to tune controllers in multivariable interactive systems in general rather than finding the best controller structure for this specific example, the use of cascade control will not be studied any further in this report.

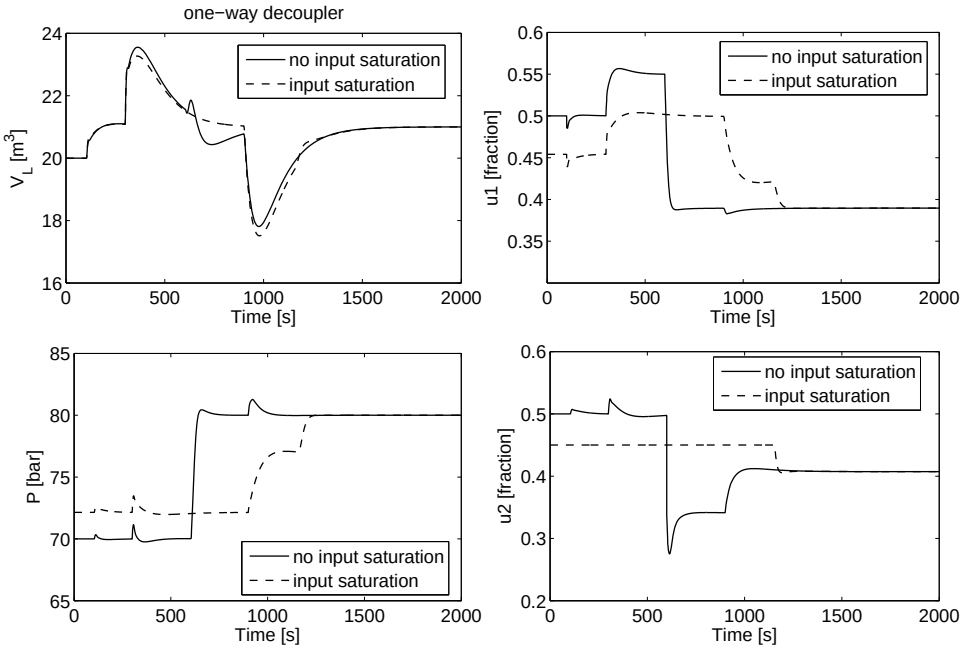

Figure 4.17: Input saturation in the level control valve u_2 with one-way decoupler.

Chapter 5

Conclusions and further work

5.1 Conclusions

In this project, an extension of the SIMC tuning rules which finds τ_c based on worst case expected conditions, has been proposed. This robust tuning rule has been tested on several cases and has proved to work very well for the different examples. This SISO rule is combined with decouplers to make a controller scheme for a multivariable coupled system which proves to be robust against changes in parameters, opening and closing loops and input saturation. In particular, one-way decouplers was concluded to be a good trade-off between simplicity and performance.

In Chapter 2 it was studied how a parameter change in the off-diagonal element in a 2×2-system would effect control with decentralized control paired on the diagonal elements. The three different decoupler methods presented in Chapter 1 was studied and tested with respect to the robustness criteria. The effect of model errors in decouplers was included as part of the worst case cases and controllers were designed based on the actual gains. For the one-way decoupler, the RGA-elements were used to find the worst case gain. With respect to the robustness criteria, only the inverted decoupler and the one-way decoupler (which is a partial inverted decoupler) managed to control the system for all cases. In particular, the ideal and simplified decouplers fail with input saturation. It was concluded that a one-way decoupler was sufficient to control the system, which is favourable because of the reduced complexity.

In Chapter 3, the robust tuning settings were first tested on three SISO cases based on a tank. For the cases sensitive to changes in operating conditions, the robust tuning parameters managed to control the systems satisfactory for all operating conditions, whereas the regular SIMC setting $\tau_c = \theta$ was too aggressive and failed in the worst case. The idea of detuning for

robustness was here applied in a systematic manner which proved to work well. Next, a multivariable interactive model of a high-pressure two-phase vessel was studied. First, a decentralized control structure was designed and the robust settings was obtained. Also in this case, the robust settings manage to control the system satisfactory for all operating conditions. By using a one-way decoupler, the system becomes robust with respect to all the robustness criteria. Thus, both the multivariable systems in Chapter 2 and 3 was controlled satisfactory with decentralized control together with a one-way decoupler.

5.2 Further work

The suggested further work is

- Include the disturbance model when designing controllers. In this project this is not handled, and the problem is just addressed.
- Try to formulate a general multivariable decentralized control tuning rule which is robust against the defined robustness criteria.
- Study systems larger than the 2×2 examples in this project.
- Study which cases a one-way decoupler is not sufficient compared to inverted decoupler.
- Compare performance of decouplers and decentralized control with MPC.

Appendix A

Sensitivity functions and stability margins

A.1 Sensitivity functions

The sensitivity function for a SISO system is defined as

$$S(s) = \frac{1}{1 + G(s)K(s)} \tag{A.1}$$

where $G(s)$ is the process and $K(s)$ is the controller (e.g. Skogestad and Postlethwaite (2005)). The sensitivity function can be used as a measure for robustness and stability margins. The complementary sensitivity function T is also of interest

$$T(s) = \frac{G(s)K(s)}{1 + G(s)K(s)} \tag{A.2}$$

where $S + T = 1$. Together they describe how much changes in the process will affect the the closed-loop system. In Seborg et al. (2004) it is shown that

$$\frac{dT/T}{dG/G} = S \tag{A.3}$$

In other words, the sensitivity function describes the ratio of change in T compared to change in G, and it is therefore desireable to have $|S|$ small (less than 1). Ideally, $|S| = 0$ is desirable, but this is not possible as can be seen from the Bode sensitivity integral Goodwin et al. (2001)

$$\int_0^\infty \ln |S(j\omega)| d\omega = 0 \tag{A.4}$$

Since $|S|$ usually is small for low frequencies and $S \to 1$ for high frequencies, it must be larger than 1 for intermediate frequencies (Skogestad and

Postlethwaite, 2005). The maximum peaks of the sensitivity and complementary sensitivity functions are

$$M_S = \|S\|_\infty = \max_\omega |S(j\omega)|; \quad M_T = \|T\|_\infty = \max_\omega |T(j\omega)| \tag{A.5}$$

In Seborg et al. (2004) the following guidelines for M_S and M_T are given

Guidelines *For a satisfactory control system, M_T should be in the range* $1.0 - 1.5$ *and M_S should be in the range* $1.2 - 2.0$.

A.2 Frequency definitions and stability margins

A.2.1 Bandwidth

The bandwidth region for a multivariable system is the frequency region from the frequency where $\bar{\sigma}(S(j\omega))$ crosses $\frac{1}{\sqrt{2}} \approx -3\,\text{dB}$ from below to the frequency $\underline{\sigma}(S(j\omega))$ crosses $\frac{1}{\sqrt{2}}$ from below (Skogestad and Postlethwaite, 2005), where $S(s)$ is the sensitivity function defined in the last section. Further, if only one frequency is desired as a bound, the bandwidth ω_B is defined as the frequency where $\bar{\sigma}(S(j\omega))$ crosses $\frac{1}{\sqrt{2}}$ from below.

A.2.2 Crossover frequency

The crossover frequency ω_c is defined as the frequency where $|L(j\omega_c)|$ first crosses 1 from above (Skogestad and Postlethwaite, 2005) where

$$L(s) = G(s)K(s)$$

A.2.3 Gain margin

The gain margin (GM) is defined as (Skogestad and Postlethwaite, 2005)

$$\text{GM} = \frac{1}{|L(j\omega_{180})|} \tag{A.6}$$

where ω_{180} is the frequency where the Nyquist curve of $L(j\omega)$ crosses the negative real axis between -1 and 0. The lower bound on GM in terms of M_S is (Skogestad and Postlethwaite, 2005)

$$\text{GM} \geq \frac{M_S}{M_S - 1} \tag{A.7}$$

A.2.4 Phase margin

Phase margin (PM) is defined as (Skogestad and Postlethwaite, 2005)

$$\text{PM} = \angle L(j\omega_c) + 180^\circ \tag{A.8}$$

where ω_c is the crossover frequency. For systems with time delay, the maximum delay before the system becomes unstable is (Skogestad and Postlethwaite, 2005)

$$\theta_{\max} = \frac{\text{PM}}{\omega_c} \tag{A.9}$$

where PM is the phase margin. The lower bound on PM in terms of M_S is (Skogestad and Postlethwaite, 2005)

$$\text{PM} \geq 2\arcsin\left(\frac{1}{2M_S}\right) \geq \frac{1}{M_S} \qquad \text{[rad]} \tag{A.10}$$

A.3 M_S calculations

With the process

$$g(s) = \frac{k}{\tau_1 s + 1} e^{-\theta s} \tag{A.11}$$

and $\tau_1 \leq 4(\tau_c + \theta)$ the SIMC PI controller becomes

$$k(s) = K_c \frac{\tau_I s + 1}{\tau_I s} = \frac{1}{k} \frac{\tau_1 s + 1}{\tau_1 s} \tag{A.12}$$

which gives

$$g(s)k(s) = \frac{1}{s(\tau_c + \theta)} e^{-\theta s} \tag{A.13}$$

The equation for $|S(j\omega)|$ is thus

$$|S(j\omega)| = \frac{1}{|1 + g(j\omega)k(j\omega)|} = \frac{1}{\left|1 + \frac{1}{j\omega(\tau_c+\theta)} e^{-j\omega\theta}\right|} \tag{A.14}$$

where $S(s)$ is the sensitivity function.

Repeating the calculations for the process

$$g(s) = \frac{k'}{s} e^{-\theta s} \tag{A.15}$$

and the controller

$$k(s) = K_c \frac{\tau_I s + 1}{\tau_I s} = \frac{1}{k'} \frac{4(\tau_c + \theta)s + 1}{4(\tau_c s + \theta)s} \tag{A.16}$$

gives

$$g(s)k(s) = \frac{4(\tau_c + \theta)s + 1}{4(\tau_c + \theta)s^2} e^{-\theta s} \tag{A.17}$$

This gives the equation for $|S(j\omega)|$

$$|S(j\omega)| = \frac{1}{|1 + g(j\omega)k(j\omega)|} = \frac{1}{\left|1 + \frac{j4\omega(\tau_c+\theta)+1}{4(\tau_c+\theta)w^2}e^{-j\omega\theta}\right|} \tag{A.18}$$

Using MATLAB, the vales for M_S given by (A.5) are calculated for (A.14) and (A.18). The values are listed in Table A.1.

Table A.1: M_s values, gain margins and phase margins.

Process $g(s)$	τ_c	M_s	lower bound GM	lower bound PM
$\frac{k}{\tau_1 s+1}e^{-\theta s}$	θ	1.59	2.69	36.7°
	0.5θ	1.92	2.09	30.2°
	0.2θ	2.39	1.72	24.2°
	0	3.13	1.47	18.4°
$\frac{k'}{s}e^{-\theta s}$	θ	1.70	2.43	34.2°
	0.5θ	2.17	1.85	26.6°
	0.2θ	2.99	1.50	19.3°
	0	4.41	1.29	12.2°

Bibliography

Edgar H. Bristol. On a new measure of interactions for multivariable process control. *IEEE Transactions on Automatic Control*, 11(1):133–134, 1966.

Chi-Tsong Chen. *Linear System Theory and Design*. Oxford University Press, Inc., third edition, 1999.

E. Gagnon, A. Pomerleau, and D. Desbiens. Simplified, ideal or inverted decoupling? *ISA Transactions*, 37(4):265–266, 1998.

Graham Goodwin, Stefan F. Graebe, and Mario E. Salgado. *Control System Design*. Prentice Hall, first edition, 2001.

J. M. Maciejowski. *Predictive Control with Constraints*. Prentice Hall, first edition, 2002.

Manfred Morari and Evanghelos Zafiriou. *Robust Process Control*. Prentice Hall, first edition, 1989.

Dale E. Seborg, Thomas F. Edgar, and Duncan A. Mellichamp. *Process Dynamics and Control*. Wiley, second edition, 2004.

F. G. Shinskey. *Process Control Systems*. McGraw-Hill, fourth edition, 1996.

Sigurd Skogestad. Simple analytic rules for model reduction and PID controller tuning. *Journal of process control*, 13:291–309, 2003a.

Sigurd Skogestad. *Prosessteknikk*. Tapir Akademisk Forlag, second edition, 2003b.

Sigurd Skogestad. Tuning for smooth PID control with acceptable disturbance rejection. *Ind. Eng. Chem. Res*, 45:7817–7822, 2006.

Sigurd Skogestad and Ian Postlethwaite. *Multivariable Feedback Control: Analysis and design*. Wiley, second edition, 2005.

Sigurd Skogestad and Erik Wolff. TANKSPILL - A Process Control Game. *CACHE News*, 32:1–4, 1991.

Harold L. Wade. Inverted decoupling- a neglected technique. *ISA Transactions*, 36(1):3–10, 1997.

Frank M. White. *Fluid Mechanics*. McGraw Hill, sixth edition, 2008.